








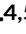



# Reconstructing formation processes at the Canary Islands indigenous site of Belmaco Cave (La Palma, Spain) through a multiproxy geoarchaeological approach

Enrique Fernández-Palacios<sup>1,2</sup>  | Margarita Jambrina-Enríquez<sup>1,3</sup>  |  
 Susan M. Mentzer<sup>4,5</sup>  | Caterina Rodríguez de Vera<sup>1</sup>  | Ada Dinckal<sup>1,2</sup>  |  
 Natalia Éguez<sup>1,2,6</sup>  | Antonio V. Herrera-Herrera<sup>1,7</sup>  |  
 Juan Francisco Navarro Mederos<sup>2</sup>  | Efraín Marrero Salas<sup>2</sup>  |  
 Christopher E. Miller<sup>4,5,8</sup>  | Carolina Mallo<sup>1,2,9</sup> 

<sup>1</sup>Archaeological Micromorphology and Biomarkers Laboratory (AMBI Lab), Instituto Universitario de Bio-Orgánica "Antonio González", Universidad de La Laguna, Tenerife, Spain

<sup>2</sup>Departamento de Geografía e Historia, UDI Prehistoria, Arqueología e Historia Antigua, Facultad de Humanidades, Universidad de La Laguna, Tenerife, Spain

<sup>3</sup>Departamento de Biología Animal, Edafología y Geología, Facultad de Ciencias, Universidad de La Laguna, Tenerife, Spain

<sup>4</sup>Institute for Archaeological Sciences, Department of Geosciences, University of Tübingen, Tübingen, Germany

<sup>5</sup>Senckenberg Centre for Human Evolution and Palaeoenvironment, University of Tübingen, Tübingen, Germany

<sup>6</sup>Department of Anthropology, University of California, Davis, California, USA

<sup>7</sup>Departamento de Química, Facultad de Ciencias, Universidad de La Laguna, Tenerife, Spain

<sup>8</sup>SFF Centre for Early Sapiens Behaviour (SapienCE), University of Bergen, Bergen, Norway

<sup>9</sup>Interdisciplinary Center for Archaeology and the Evolution of Human Behaviour (ICArEHB), Universidade do Algarve, Campus de Gambelas, Faro, Portugal

## Correspondence

Enrique Fernández-Palacios, Archaeological Micromorphology and Biomarkers Laboratory (AMBI Lab), Instituto Universitario de Bio-Orgánica "Antonio González", Universidad de La Laguna, San Cristóbal de La Laguna 38206, Tenerife, Spain.  
 Email: [efernand@ull.edu.es](mailto:efernand@ull.edu.es)

Scientific editing by Sarah C. Sherwood.

## Funding information

Spanish Ministry of Universities, Grant/Award Number: FPU19/02379; Fundación Caja Canarias and "La Caixa" (2018PATRI19)

## Abstract

The indigenous populations of La Palma (Canary Islands), who arrived on the island from Northwest Africa ca. 2000 years B.P., were predominantly pastoralists. Yet, many aspects of their subsistence economy such as the procurement, management, and use of wild plant resources remain largely unknown. To explore this, we studied the 600–1100-year-old archaeological site of Belmaco Cave, which comprises a stratified sedimentary deposit representative of a *fumier*. Here, we present a high-resolution, multiproxy geoarchaeological study combining soil micromorphology, lipid biomarker analysis, X-ray diffraction,  $\mu$ -X-ray diffraction,  $\mu$ -X-ray fluorescence, Fourier transform infrared spectroscopy, and  $\mu$ -Fourier transform infrared spectroscopy, to characterize formation processes and explore plant sources. Recurrent goat/sheep habitation and maintenance activities are represented by interstratified layers of unburned dung, charcoal-rich sediment, and dung ash. Lipid biomarker data show a herd diet mainly composed of herbaceous plants, which is key to understanding the mobility of indigenous shepherds. Our results also revealed an

This is an open access article under the terms of the Creative Commons Attribution-NonCommercial-NoDerivs License, which permits use and distribution in any medium, provided the original work is properly cited, the use is non-commercial and no modifications or adaptations are made.

© 2023 The Authors. *Geoarchaeology* published by Wiley Periodicals LLC.

unusual suite of authigenic minerals including hazenite, aragonite, and sylvite, possibly formed through diagenetic processes involving interaction between ash, dung, urine, volcanogenic components, and bacterial activity, coupled with arid and alkaline conditions. Our study shows the potential of a multiproxy approach to a *fumier* deposit in a volcanogenic sedimentary context.

#### KEYWORDS

*Fumier*, lipid biomarkers, micromorphology, *n*-alkanes,  $\mu$ -FTIR,  $\mu$ -XRD,  $\mu$ -XRF

## 1 | INTRODUCTION

During the initial settlement of the Canary archipelago, populations arriving from the African continent encountered numerous challenges across radically different landscapes. These new landscapes included volcanic terrains, such as calderas and ravines, where new populations encountered raw materials including obsidian and basalt. There were a variety of new ecosystems with unknown endemic flora and fauna, and the new scenario implied the loss of important continental resources, such as flint, metals, big game, and rivers. The accompanying sheep and goat herds also had to adapt to the new environmental conditions. As a result, the settlers and their herds dramatically transformed the landscape, likely accelerating erosion and ecological perturbation processes, including species extinctions and extirpations (Fernández-Palacios et al., 2016; de Nascimento et al., 2009, 2016, 2020; Ravazzi et al., 2021).

La Palma, the north-western-most island of the Canary archipelago (Spain), constitutes an exceptional scenario to study such adaptation processes. The indigenous inhabitants of La Palma, known as the Auaritas, were genetically related to North-West African Amazigh populations (Fregel et al., 2009). The earliest documented indigenous site in La Palma dates to 260–450 cal. C.E. (Morales et al., 2017) and archaeological evidence indicates continuous presence of the Auarita population until the arrival of European colonizers in the island at the end of the 15th century A.D.

La Palma has a rugged orography with common escarpments and gorges that are considered difficult for farming but suitable for herding goats, and nowadays fodder sources are diverse and abundant. Information concerning indigenous subsistence strategies in La Palma has been gathered from archaeological and ethnohistorical records. The latter, written by European explorers in the 15th and 16th centuries, state that the Auaritas relied on animal husbandry and plant gathering, which suggests an absence of agriculture (Abreu, 1977; Cioranescu, 2004). Zooarchaeological investigations have shown that the livestock consisted of goats (*Capra hircus*), sheep (*Ovis aries*), and pigs (*Sus domesticus*); domesticated animals introduced by the first inhabitants (Pais Pais, 1996a). Scattered archaeological and ethnographic data document numerous herding sites in the highlands, pointing to a

reliance on pastoralism (Martín Rodríguez, 1992; Pais Pais, 1996a, 1996b, 2008). On the other hand, the localized presence of barley (*Hordeum vulgare*), wheat (*Triticum durum*), lentils (*Lens culinaris*), and fava beans (*Vicia faba*) in archaeological deposits suggests that agriculture also played a role in indigenous subsistence practices (Morales, 2003; Morales & Gil, 2014; Morales et al., 2007, 2009, 2014). Nevertheless, this evidence is isolated, as only a few cultivar seed remains have been found in only two archaeological sites, and Morales et al. (2014) highlight the prevalence of pastoral subsistence in La Palma. Further investigation of indigenous archaeological contexts in La Palma is necessary to gain insight into the Auarita subsistence economy. Given the likely importance of animal husbandry, a focus on indigenous herding practices is particularly called for to explore traditions regarding livestock management, maintenance of the herding sites, fodder sources, and their procurement strategies.

One way to approach these issues is through the geoarchaeological study of burnt stabling deposits or *fumiers*. Natural caves and rockshelters have traditionally been used as seasonal pens for livestock from the Neolithic until the Bronze Age in the Mediterranean region, resulting in the formation of thick stratified deposits representing recurrent anthropogenic stabling activity. Throughout their formation, these stabling deposits were periodically burnt to eliminate parasites, sanitize penning areas, and reduce accumulated dung volume. The resulting burnt stratified sequence is commonly referred to as *fumier* (Angelucci et al., 2009; Brochier et al., 1992; Brochier, 1983a, 1983b, 1991, 1996, 2002). From a macrostratigraphic perspective, *fumiers* are characterized by an alternation of successive, well-bedded, thin layers of variable color and are usually poor in archaeological materials (Angelucci et al., 2009; Fernández Eraso & Polo Díaz, 2009).

*Fumiers* have often been approached through archaeological soil micromorphology, which provides a set of indicators to assess formation processes. From a micromorphological perspective, *fumiers* display (1) a brown layer formed of mostly unaffected dung residues (which can include other biogenic or geogenic materials), (2) a black layer showing partially charred dung and other organic materials, and (3) a white/gray layer of ashed dung or a combination of wood and dung ashes. The brown layer (1) may include plant material introduced as bedding to prepare the ground surface for animal occupation and represents the stabling event, followed by the black

and white/gray layers (2 and 3), or the effects of burning, which penetrate down into the sediment beneath (Angelucci et al., 2009; Égüez et al., 2016; Macphail et al., 1997; Polo-Díaz et al., 2014, 2016; Polo-Díaz, 2010). Nevertheless, using soil micromorphology as a stand-alone technique in the study of *fumiers* also has disadvantages. One of them is the difficulty in identifying the diagenetic processes that are often associated with this kind of deposit (Polo Díaz & Fernández Eraso, 2010). Complementary inorganic geochemistry techniques such as Fourier transform infrared spectroscopy (FTIR), X-ray diffraction (XRD), and scanning electron microscopy (SEM) have been valuable sources of information (Brochier et al., 1992; Burguet-Coca et al., 2020; Cabanes et al., 2009). However, diagenetic pathways of *fumier* components in deposits associated with volcanic settings remain unexplored.

Another disadvantage is the difficulty in identifying plant sources, which are a key component of stabling deposits and may include fodder remains, digested plants within the dung pellets, bedding, and fuel. Multiproxy studies using phytoliths, pollen, calcium oxalates, ash pseudomorphs, charcoal, and other plant macroremains analyses have provided valuable information on plant sources and possible livestock diets (Allué et al., 2009; Alonso-Eguíluz, 2012; Cabanes et al., 2009; Delhon et al., 2008; Expósito & Burjachs, 2016; Rodríguez et al., 2016; see also Delhon et al., 2023 and references therein), many of them following or combining these proxies with micromorphological analysis (Alonso-Eguíluz et al., 2016; Burguet-Coca et al., 2020; Euba et al., 2016; Lancelotti et al., 2014; Polo-Díaz et al., 2016). Alternatively, micromorphology could be combined with lipid biomarker analysis, with certain types of lipids serving as proxies for plant sources. Lipids are the most resistant biomolecules in the archaeological record, making them extremely useful proxies in many different contexts for paleoenvironmental and paleodietary research (Peters et al., 2007). Among the numerous lipid compounds preserved in organic-rich dung deposits, *n*-alkanes are the most resistant to microbial degradation (Volkman et al., 1998). Alkanes are hydrocarbon molecules that form linear chains of carbon atoms (*n*-alkanes) and derive from epicuticular waxes of vascular plants (Eglinton & Hamilton, 1967). Different plant species produce a characteristic, identifiable pattern and quantity of *n*-alkanes. Therefore, these molecular compounds, which persist in animal excrements after plant consumption, can be used to reconstruct the animals' diet (Dove & Mayes, 1996, 2005).

To our knowledge, studies reporting lipid biomarker data from archaeological *fumiers* are still scarce and mostly focus on sterols and bile acids (Gea et al., 2017; Vallejo, Gea, Gorostizu-Orkaiztegi, et al., 2022). *n*-Alkane biomolecular data have been used to address contemporary pastoral activity in eastern Mongolia (Égüez & Makarewicz, 2018; Égüez et al., 2022), North Africa (Égüez et al., 2018), and the Pyrenees (Pescini et al., 2023) providing a valuable reference for herd diet and taphonomic processes associated with sheep and goat dung deposits, albeit not from archaeological *fumiers*. Archaeo- and rock magnetic data from archaeological *fumiers* have indicated maximum burning temperatures of 400–500°C in carbonaceous facies and 600–700°C in ash layers

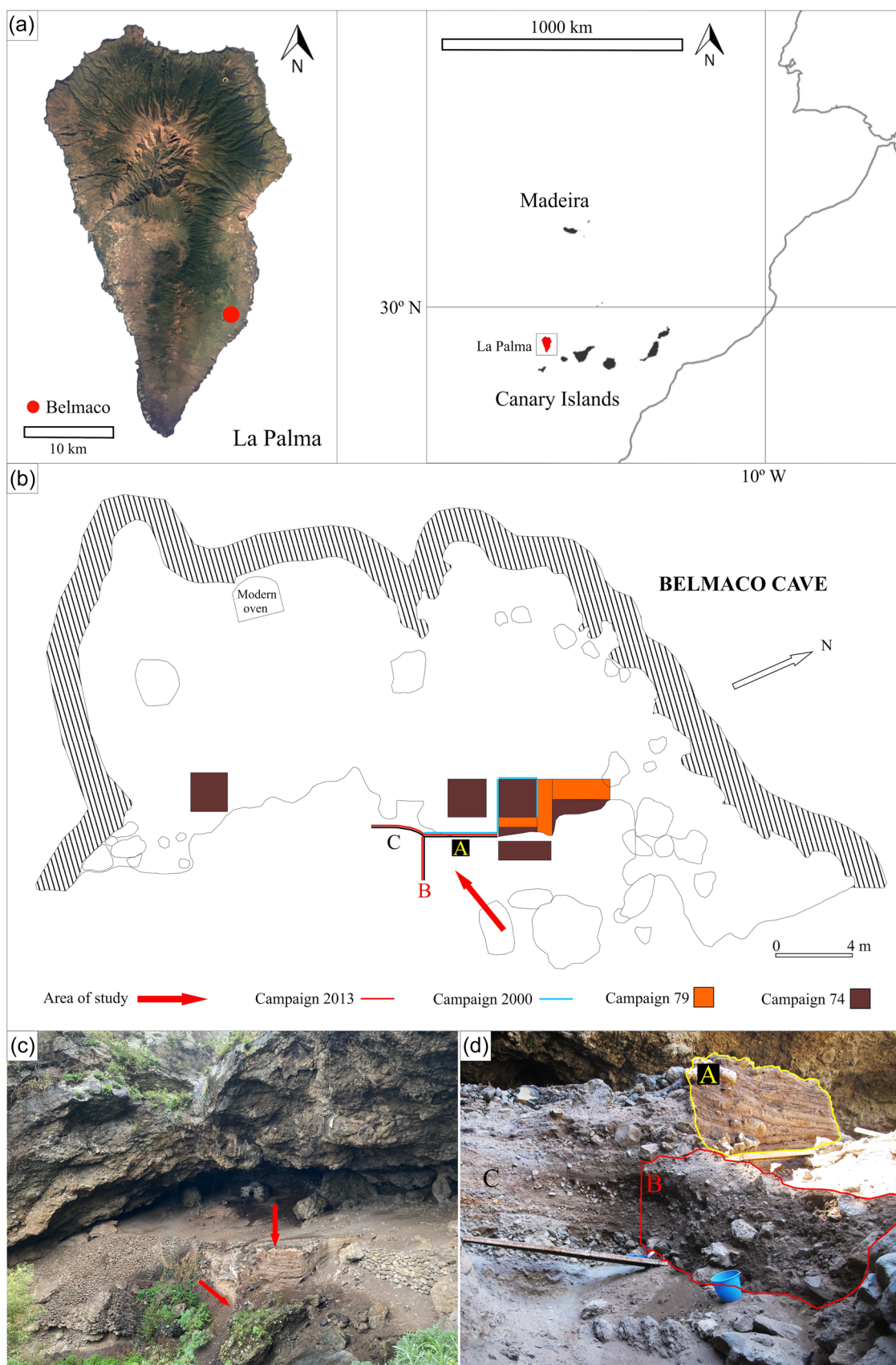
(Burguet-Coca et al., 2022; Carrancho et al., 2012, 2016). Controlled laboratory heating sequences have shown that plant *n*-alkanes are well preserved up to 350°C (Jambrina-Enríquez et al., 2018; Wiesenberg et al., 2009) and there is potential for successful application of *n*-alkane biomarkers in archaeological *fumier* deposits. A recent livestock diet study using excremental *n*-alkanes in the Neolithic–Bronze Age *fumier* sequence of El Mirador (Burgos, Spain) showed good biomarker preservation in partially and completely burnt layers (Vallejo, Gea, Massó, et al., 2022).

In this study, we used a multiproxy approach to formation processes at the Belmaco Cave *fumier*, a key indigenous site in La Palma dated to between the 9th and the 15th centuries A.D. (Marrero Salas et al., 2016). We applied soil micromorphology and *n*-alkane biomarker analyses to characterize depositional sources and the formation history of the sequence, approach herd diet composition and its changes over time, and explore combustion temperatures. We complemented these data with XRD,  $\mu$ -XRD,  $\mu$ -XRF, FTIR, and  $\mu$ -FTIR analyses of selected samples to elucidate diagenetic processes in a volcanogenic sedimentary context.

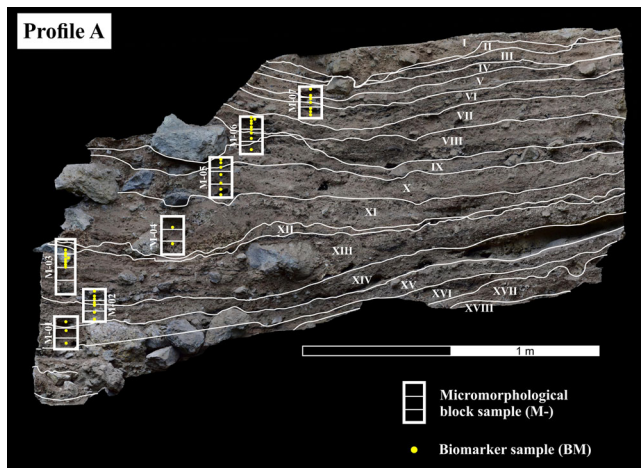
## 2 | MATERIALS AND METHODS

### 2.1 | Site background

Belmaco Cave (Villa de Mazo) is located in south-eastern La Palma, at an altitude of 362 m a.s.l., within Las Cuevas Ravine (28°34'40" N, 17°46'36" W) (Figure 1). Concerning the geological setting, it is found in the eastern flank of the Cumbre Vieja volcanic Massif (Carracedo et al., 2015). The ravine exposed a pre-LGM Pleistocene basalt bed in which the Belmaco Cave structure is found. The landscape surrounding the ravine is made up of younger, post-LGM Pleistocene basalt beds, which extend from the Cumbre Vieja summit along the eastern slope of the island and down to the coast. Belmaco Cave is shallow, around 10 m deep, and sunlit, which makes it more of a rockshelter. Its formation is volcanogenic, possibly a blister or pressure-ridge cave, commonly associated with massive basalt lava flows (Mentzer, 2016). The first excavations in the northern part of the cave recovered a rich archaeological assemblage including pottery, lithic tools on basalt, ornaments, sheep/goat bone fragments, shells, wooden artifacts, post holes, and fireplaces (Diego Cuscoy, 1962; Navarro Mederos et al., 2013; Pais Pais, 2017). Subsequent excavation seasons (1974; 1979–1980; 2000) focused on the central area, and the latest were geared at assessing the preservation of the stratigraphic profiles, which had been affected by many tourist visits to the site, lizard and rodent activity, and torrential floods (Hernández Pérez, 1999; Morales et al., 2007). The presence of a *fumier* at the site was proposed based on salvage archaeological fieldwork in 2013, which yielded scarce archaeological remains (Marrero Salas et al., 2016). This campaign focused on analyzing three stratigraphic profiles in the central area of the cave. Profile A (Figure 1), which was already exposed since the 70s, displays a 2.8 m long stratigraphic sequence,



**FIGURE 1** (a) Geographic location of La Palma and Belmaco Cave archaeological site. (b) Site map indicating the area of study. (c) General view of the Belmaco Cave rockshelter and location of the sedimentary deposit under investigation (arrows); (d) Location of the two perpendicular Profiles (A and B) in the central area of the cave. [Color figure can be viewed at [wileyonlinelibrary.com](https://onlinelibrary.wiley.com/doi/10.1002/gea.21972)]



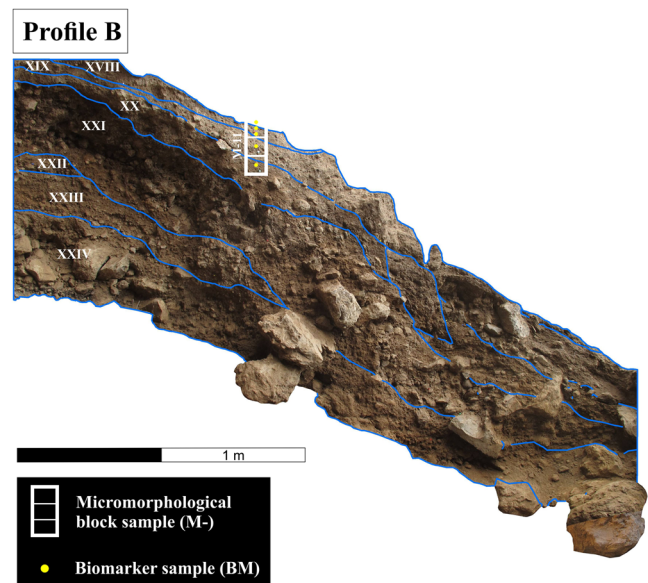
**FIGURE 2** Photogrammetry model of Profile A showing stratigraphic units I–XVIII, and micromorphology and lipid biomarker sample provenience. The top of the sequence (SU 0; 0–15 cm; a recent, anthropogenic stone bed) was not included in this model. Thin sections corresponding to each micromorphological block are numbered from top to bottom (e.g., M-04/1 = upper thin section; M-04/2 = middle; M-04/3 = lower). [Color figure can be viewed at [wileyonlinelibrary.com](https://onlinelibrary.wiley.com)]

and constitutes a central topic of this study. Profiles B and C (Figure 1) were exposed by runoff and ravine flank collapses in 2012, which motivated the intervention in 2013. Profile B is also included in this study (1.7 m), and represents the lower part of the stratigraphic sequence. Stratigraphic units (SU) were described during the 2013 campaign. Radiocarbon dating was performed on bone remains from three units, ordered from lowest to highest, with SU XXI ranging from 882 to 1015 cal. A.D. (Beta382867: 1110 ± 30 B.P.); SU XVI ranging from 1028 to 1172 cal. A.D. (Beta382866: 940 ± 30 B.P.); and SU III ranging from 1305 to 1419 cal. A.D. (Beta382865: 580 ± 30 B.P.) (Marrero Salas et al., 2016).

## 2.2 | Micromorphology

Eight intact, oriented block samples for micromorphological analysis were extracted: seven from Profile A (Figure 2) and one from Profile B (Figure 3). Micromorphology blocks were processed by Thomas Beckmann into 9 cm × 6 cm × 30 μm thin sections. A total of 25 thin sections were observed and analyzed in plain polarized light (PPL) and cross-polarized light (XPL) using two petrographic microscopes (Nikon E600-POL and Nikon AZ100).

The microfacies approach to soil micromorphology (Courty, 2001) is used in this study to facilitate the study of Belmaco's formation processes. Individually defined microfacies units (MFU), are grouped into microfacies types (MFT), based on specific combinations of micromorphological components and microstructures. Identification and description of micromorphological features follow standard guidelines defined by Stoops (2021), Nicosia and Stoops (2017), and Stoops et al. (2018).



**FIGURE 3** View of Profile B showing the lower units of the stratigraphic sequence (XVIII–XXIV), and micromorphology and lipid biomarker sample provenience. [Color figure can be viewed at [wileyonlinelibrary.com](https://onlinelibrary.wiley.com)]

## 2.3 | *n*-Alkanes

For the study of lipid biomarkers, 48 bulk sediment samples (BM) were collected with sterilized metal tools and nitrile gloves from each macroscopically visible facies within the negatives of the micromorphological block samples (43 on Profile A and 5 on Profile B) (Figures 2 and 3; see Supporting Information for sample ID and corresponding depth, Supporting Information: Table S2). For each visible facies, we gathered around 20 g of sediment. A control sample was also collected outside of the sequence (20 m away) from the natural geological stratigraphy (1.5 m below the beginning of the *fumier* sequence). These were packed in aluminum foil and stored at –20°C to avoid bacterial degradation, until processing at the Archaeological Micromorphology and Biomarkers Laboratory (University of La Laguna) could commence. As a reference for the *n*-alkane study, four fresh plant species from different vegetation belts were also collected corresponding to the following taxa: *Lotus hillebrandii* (Fabaceae; pine forest; 28°31'37" N, 17°51'07" W), *Hypparrhenia hirta* (Poaceae; coastal scrub; 28°34'47" N, 17°52'47" W), *Bituminaria bituminosa* (Fabaceae; thermophilous woodlands and pine forest; 28°30'05" N, 17°50'27" W), and *Echium brevirame* (Boraginaceae; transition coastal scrub–thermophilous woodlands; 28°33'07" N, 17°47'21" W). Due to the high degree of disturbance of the original vegetation immediately surrounding the site, specimens of these species were collected within a radius of 10 km around Belmaco. The use of these particular taxa as fodder has been documented ethnographically and archaeologically (del Arco, 1993; Pais Pais, 1996a). This will help determine the OM sources in the *fumier* sequence, assuming that

the *n*-alkane distribution of the current vegetation is representative of past vegetation communities.

*n*-Alkane extraction protocol followed that established by Herrera-Herrera and Mallol (2018), Leierer et al. (2019), and Connolly et al. (2019). In summary, the total lipid was extracted using a 9:1 v/v DCM:MeOH mixture. *n*-Alkanes were separated using SPE column chromatography, analyzed by gas chromatography–mass spectrometry, and subsequently quantified using calibration curves. A detailed explanation of extraction and analysis procedures can be found in Supporting Information: Text S1. The *n*-alkane concentration is expressed as  $\mu\text{g}$  per gram of dry sample ( $\mu\text{g/gds}$ ).

## 2.4 | Total, inorganic, and organic carbon analyses

The organic carbon content was determined for all 48 sediment samples (BM), distinguishing between total carbon (TC), total inorganic carbon (TIC), and total organic carbon (TOC) with a LECO SC 144DR furnace at Instituto Pirenaico de Ecología (IPE-CSIC), Spain.

## 2.5 | $\mu$ -X-ray fluorescence ( $\mu$ -XRF)

To explore the elemental composition of the MFTs and of certain unidentified crystals, we carried out  $\mu$ -XRF on 11 chips or resin-impregnated slabs left over from thin section production (M-11/3, M-11/2, M-11/1, M-07/2, M-07/1, M-05/1, M-04/1, M-03/1, M-02/2, M-01/2, and M-01/1). These are mirror images of the micro-morphological thin sections.  $\mu$ -XRF scanning was carried out at the Microanalytics Laboratory (Institute for Archaeological Sciences) at the University of Tübingen, Germany. A Bruker M4 Tornado was used for elemental map scanning. Elemental maps for the following elements were produced: Al, Ca, Cu, Fe, K, Mg, Mn, Na, P, S, Si, Ti, and Zn. The instrument settings used for mapping were a beam power of 30 W (50 kV tube voltage and 600  $\mu\text{A}$  tube current), use of both detectors, a spot size of  $\sim 20 \mu\text{m}$ , and a spot spacing of 8–60  $\mu\text{m}$  depending on the resolution desired. Dwell times per pixel of 10 ms up to 100 ms were used, depending on the elements of interest. The analyses were carried out under full vacuum. The elemental maps were only analyzed qualitatively, that is, presence/absence and spatial distribution of elements.

## 2.6 | X-ray powder diffraction (XRD)

X-ray diffraction was performed on sediment samples BM 7-1, BM 7-4, BM 4-2, and BM 2-2 because the micromorphological analysis indicated a high concentration of unidentified crystals in the layers corresponding to these sediment samples. After homogenization, power diffractograms were recorded between  $2\theta^\circ = 5^\circ$  and  $80^\circ$  (working conditions:  $0.02^\circ/\text{step}$ ,  $996.54 \text{ s}/\text{step}$ , 40 mA) using a *Bragg-Brentano* Panalytical X'Pert Pro

diffractometer (K line of a Cu anode, no incident beam monochromator). The sample holder was in constant rotation during the analysis. Mineralogical identification was carried out using Highscore Plus software (version 4.9) and the PDF4+2021 database. A semiquantitative analysis was carried out based on the normalized reference intensity ratio (RIR) values (or I/Ic values) and the scale factors, which allow determining estimated mass fractions of the identified mineralogical phases (Chung, 1974). Amorphous phases are not considered. Some phases have no available RIR values displaying no % data.

## 2.7 | $\mu$ -XRD

$\mu$ -X-ray diffraction was performed on a single chip (M-01/2), where several clusters of potentially phosphatic minerals were targeted. A Bruker D8 Discover  $\Theta/\Theta$  GADDS micro-diffractometer was used. This was equipped with a Co-sealed tube running at 30 kV/30 mA, a HOPG-primary monochromator, and a  $50 \mu\text{m}$  monocapillary optic, with rotation. Phase identification was conducted using the PDF-2 database and Match! software.

## 2.8 | Fourier transform infrared spectroscopy (FTIR)

FTIR was used as a supplemental analysis for select samples BM 7-1 and BM 4-2 collected as bulk sediment in 2 mL plastic vials. FTIR measurements were carried out using a Cary 630 (Agilent Technologies) portable FTIR with a diamond crystal attenuated total reflectance (ATR) module. Spectra were measured using the MicroLab software, with spectra generated from 32 coadded scans at  $4 \text{ cm}^{-1}$  resolution over a spectral range of  $400\text{--}4000 \text{ cm}^{-1}$  with background measurements taken before every sample. The resulting spectra were compared to references from the RRUFF ATR spectral database (Lafuente et al., 2016), the Kimmel Center KBr spectral database (<https://centers.weizmann.ac.il/kimmel-arch/infrared-spectra-library>), and the INA (University of Tübingen) ATR spectral database.

## 2.9 | $\mu$ -FTIR

$\mu$ -FTIR analyses were conducted using a Cary 610 (Agilent Technologies) microscope attached to a Cary 670 laboratory bench FTIR. The spectra were collected from the surfaces of the resin-indurated chips (M-01/2 and M-04/3) left over from thin-section production. Reflectance spectra were collected with 64 or 128 coadded scans at  $2 \text{ cm}^{-1}$  resolution over a spectral range of  $400\text{--}4000 \text{ cm}^{-1}$  and reported as %Reflectance, with a variable analytical area determined by apertures. Measurements were also conducted using a diamond crystal ATR objective with an analytical area of approximately  $100 \mu\text{m}$ . The absorbance spectra were collected with 36 coadded scans at  $4 \text{ cm}^{-1}$  resolution and a

spectral range of 400–4000  $\text{cm}^{-1}$ . The reflectance spectra and ATR spectra were compared to the same reference databases listed above, as well as peak positions reported in publications. A Kramers–Krönig transformation was applied in some cases to better compare reflectance peak positions to published transmission peak positions.

### 3 | RESULTS

#### 3.1 | Micromorphology

##### 3.1.1 | Components, microstructure, porosity, postdepositional processes

The studied sedimentary sequence is composed of sand/gravel-sized detritic basalt, pumice, and volcanic glass. These

components are poorly sorted and are present throughout the sequence. Numerous basalt fragments display dotted alteration indicating mild weathering. The proportion of detritic material increases in block sample M-11 (Profile B). Anthropogenic and biogenic components include wood charcoal, charred seeds, calcified plant remains, bone, pottery, and both charred and unburned coprolites (Table 1 and Figure 4). Opaline phytoliths, calcium oxalate crystals, and fecal spherulites are abundantly found throughout the sequence. Two types of (possible) authigenic secondary minerals stand out: one type forming clusters or nodules in voids, and another forming laths within the sedimentary matrix (Table 1 and Figure 5).

The general groundmass varies between fresh, unburned dung areas composed of disintegrated dung pellets and large quantities of unaltered fecal spherulites (see Figure 4) in an open to single space porphyric  $c/f_{20\mu\text{m}}$ -related distribution and dung ash areas characterized by a variable open porphyric to gefuric  $c/f_{20\mu\text{m}}$ -related distribution. The fine mass of

**TABLE 1** Micromorphological descriptions of the main components identified throughout the sequence.

| Component   | Description   |
|---|---|
| Wood charcoal   | Common to dominant in black/carbonized layers; few in unburned and ashy layers; fine gravel to medium sand-sized; angular to rounded, mostly subrounded; most of the fragments are dicotyledonous species (broad-leaf trees), only little presence of conifer fragments; degradation and loose of structure of many fragments |
| Charred seeds   | Very few, only in sample M-07/2; burned; gravel-sized; rounded  |
| Pine needles  | Few embedded in dung ash and scattered in carbonized layers of M-02/1, M-03/2, M-03/4, M-06/2, and M-07/2; coarse sand-sized; black-hook shape in cross-section; subrounded   |
| Bones   | Very few in samples M-02/1, M-04/1, and M-05/3; from reptile or fish; unburned; gravel-sized; angular to subrounded   |
| Pottery   | Very few, only in sample M-06/1; gravel-sized; subrounded   |
| Opaline phytoliths  | Common to frequent in unburned dung-dominated areas; silt-sized   |
| Coprolite fragments                                       | Frequent in most samples; usually fragmented; fibrous and convoluted; sometimes burned and/or deformed, especially in unburned dung layers and black layers; coarse/very coarse sand-sized; subrounded to rounded   |
| Charred plant remains                                     | Common to very dominant in black/carbonized layers; degraded structure of plant tissue; medium sand to gravel-sized; subangular to subrounded   |
| Authigenic (evaporitic) crystals forming nodules/clusters | Dominant in unburned dung-dominated areas, while in ashy and charred areas, it is few to common; fine sand to fine gravel-sized; angular; lenticular and tabular crystals, sometimes forming rosettes; colorless in PPL and sky blue to dark blue interference colors in XPL  |
| Lath-shaped crystals                                      | Dominant in ash-dominated areas; medium to coarse sand-sized; lath/needle-shaped, angular; dark gray in PPL; high birefringence in XPL  |
| Calcium oxalate crystals/druses                           | Common in unburned dung layers; somewhat bigger in size compared to dung spherulites, still silt-sized  |
| Fecal spherulites   | Very dominant throughout the sequence, except in certain ashy areas; present both unaltered (unburned dung) and darkened spherulites (dung ash); silt-sized (typically 5–20 $\mu\text{m}$ ); calcitic; sometimes forming crusts or laminations  |
| Avireptilian uric acid spheres                            | Few to common in layers showing low-temperature thermal alteration; similar structure to fecal spherulites but with a higher refractive index; silt-sized (typically 2–10 $\mu\text{m}$ ); usually forming crusts or laminations  |
| Calcium carbonate plant pseudomorphs                      | Dominant in plant ash deposit in M-07/1; calcitic; medium sand to gravel-sized; angular to subrounded   |

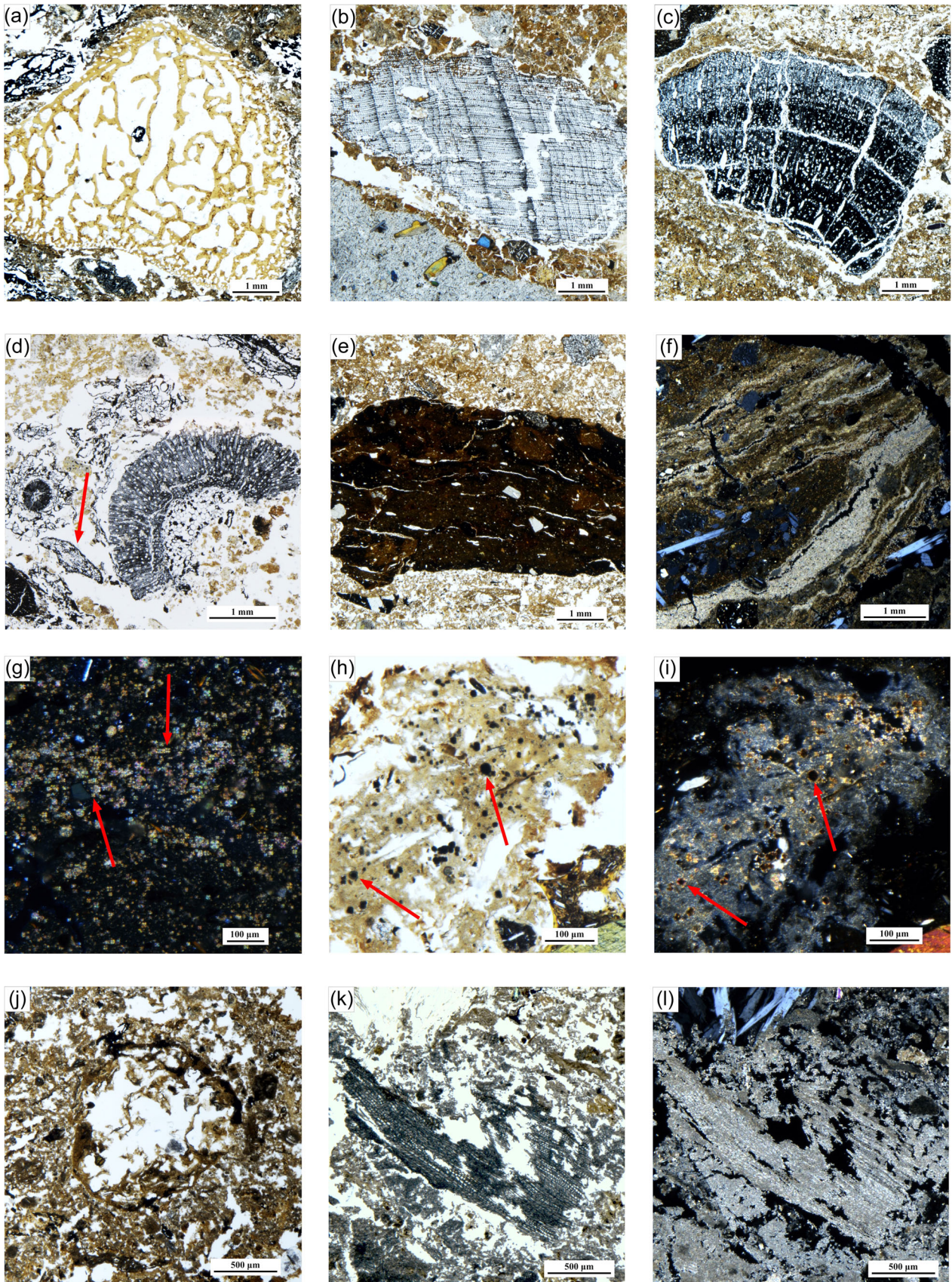
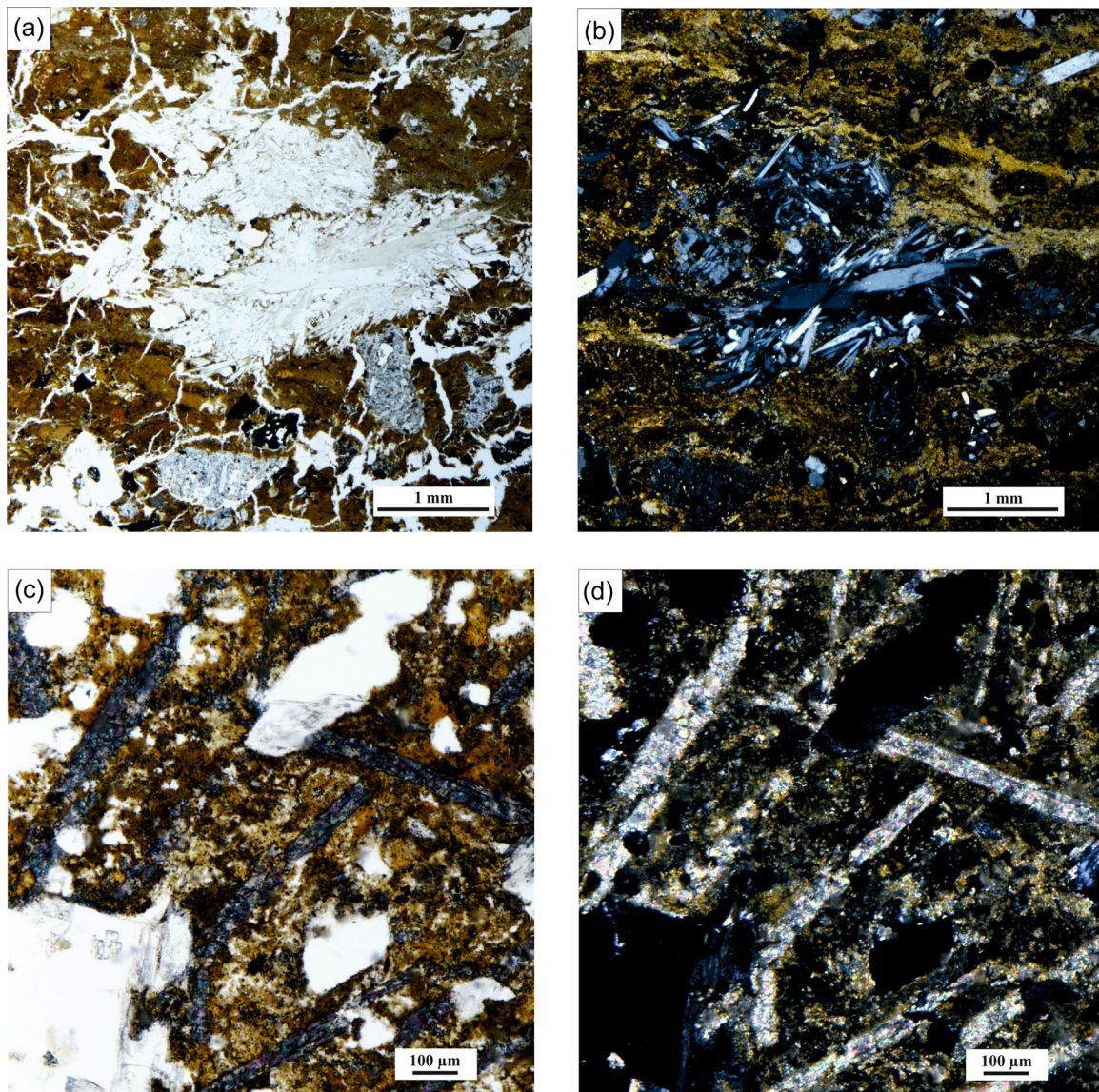


FIGURE 4 (See caption on next page).





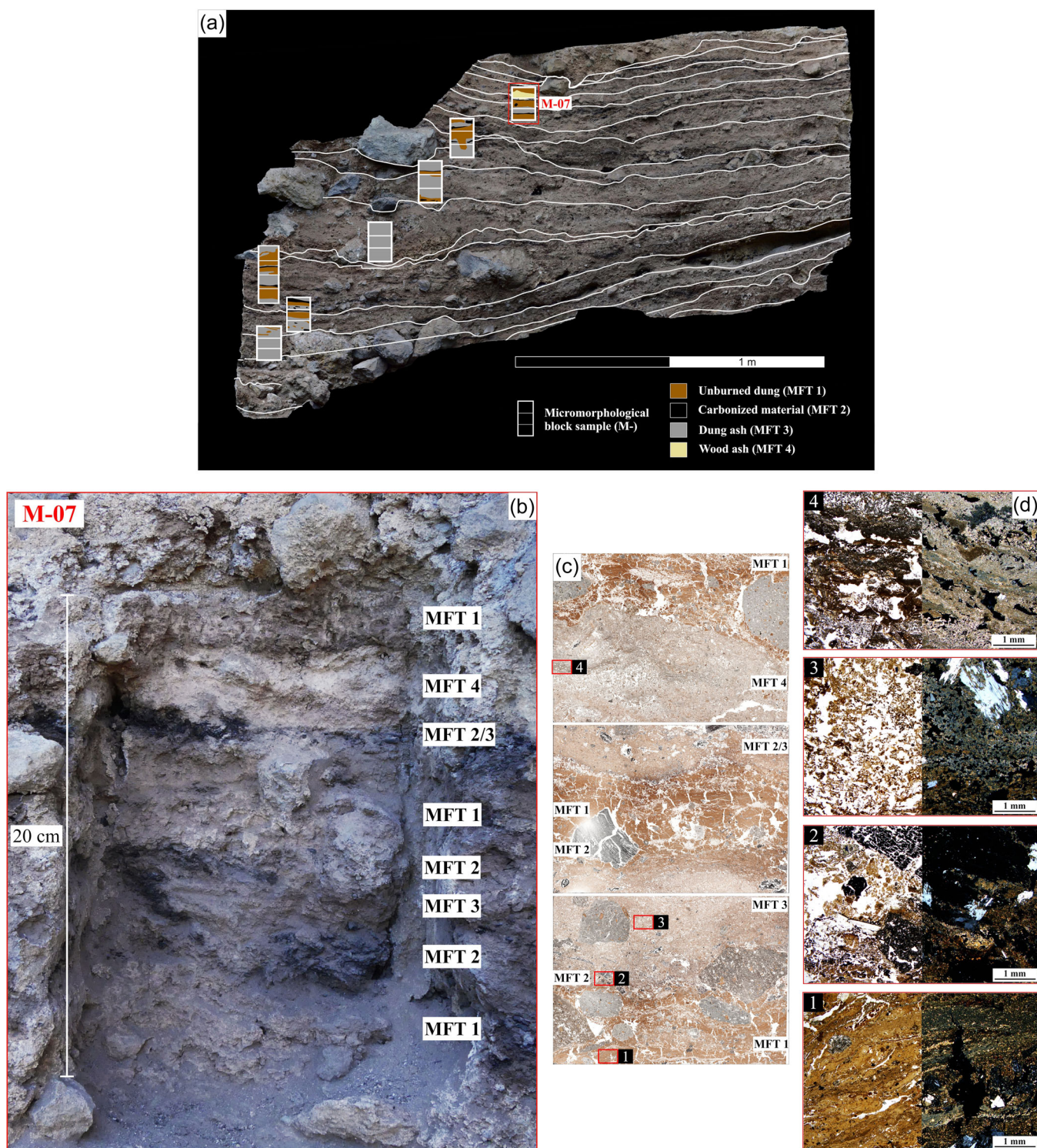
**FIGURE 5** Authigenic secondary minerals identified through micromorphology. (a) Authigenic evaporitic crystal cluster forming in the voids of an unburned dung layer (PPL). Identified as hazenite in combination with techniques for mineralogical analysis. (b) Same as (a) in XPL. (c) Lath-shaped crystals within dung ash matrix (PPL). Identified as aragonite in combination with mineralogical techniques. (d) Same as (c) in XPL. PPL, plain polarized light; XPL, cross-polarized light. [Color figure can be viewed at [wileyonlinelibrary.com](https://onlinelibrary.wiley.com/terms-and-conditions)]

the ashy areas varies between an undifferentiated and compacted matrix, appearing darker in XPL, with a calcitic–crystallitic and more open matrix (Figures 6 and 7). The microstructure of the ashy areas is spongy (fibrous) and crumbly with vughs. Unburned dung layers show a variably platy, channel or massive microstructure with channels, vertical fissures, planes, and vughs (Figures 6 and 7).

### 3.1.2 | MFUs and MFTs

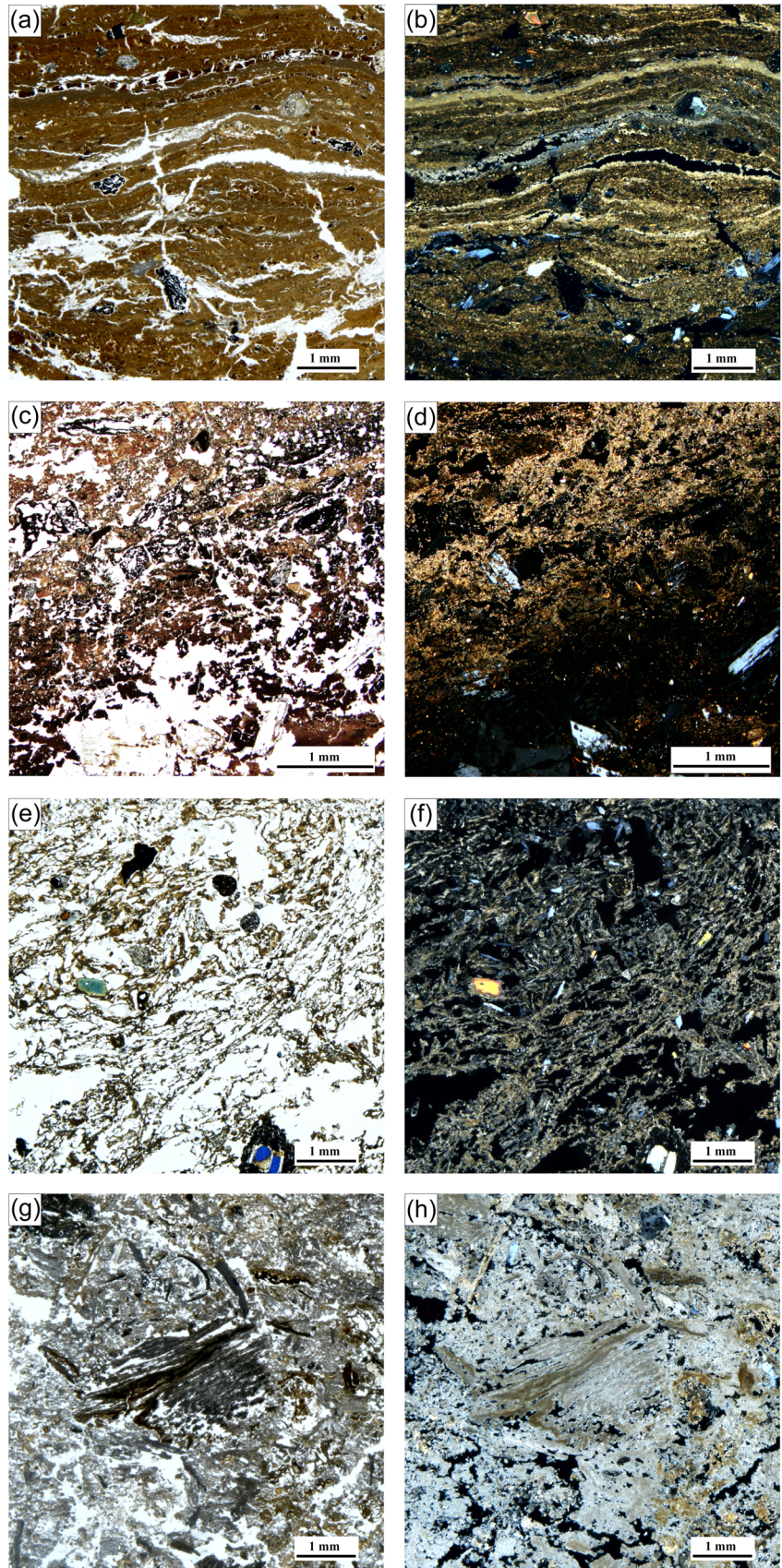
According to their stratigraphic position and previously described features (components, microstructure, and porosity) a total of 45 MFUs were identified. These are presented in Supporting Information: Table S1 and Figure S6. The MFUs have been

**FIGURE 4** Selected anthropogenic and biogenic microscopic components: (a) Bone fragment (PPL). (b) Conifer charcoal (PPL). (c) Broad-leaf tree charcoal (PPL). (d) Pine needle cross-section marked by red arrow (PPL). Note black hook shape. (e) Pottery fragment (PPL). (f) Spherulitic crusts made of fecal spherulites and avireptilian uric acid spheres (MFT 1) (XPL). (g) Detail of unaltered fecal spherulites marked by red arrows (MFT 1) (XPL). (h) Darkened fecal spherulites marked by red arrows (MFT 3) (PPL). (i) Same as (h) in XPL. (j) Goat/sheep coprolite fragment (PPL). Note its convoluted pattern. (k) Wood ash with visible tracheid (PPL). (l) Same as (k) in XPL. PPL, plain polarized light; XPL, cross-polarized light.



**FIGURE 6** (a) Distribution of microfacies types (MFTs) across Profile A. (b) Detail of micromorphology block M-07 indicating MFTs; (c) Thin-section scans (8×6 cm) of M-07/1 (upper), M-07/2 (middle), and M-07/3 (lower) (PPL) showing corresponding MFTs; (d) Photomicrographs illustrating the main features of each MFT (PPL, left; XPL, right). 1: massive, unburned dung with few planes and vughs in MFT 1; 2: charred plant fragments in MFT 2, at the contact between unburned dung and dung ash. Evaporitic crystals visible in XPL; 3: Dung ash in MFT 3. Note the spongy microstructure and darkened fecal spherulites. Evaporitic crystals visible in XPL; 4: plant ash in MFT 4, exhibiting an alternating vughy and crumbly microstructure. Note the high birefringence and calcitic-crystallitic b-fabric in XPL (see Supporting Information: Figure S16 for a field view of this ashy facies). PPL, plain polarized light; XPL, cross-polarized light.

**FIGURE 7** Microfacies types (MFTs) identified in the micromorphological samples. (a) MFT 1: Unburned dung matrix with abundant unaltered calcareous dung spherulites. The microstructure is compact, microlaminated, and undulating, dominated by vertical fissures and planar voids (PPL). (b) Same as (a) in XPL. The difference between the high birefringence laminations and darker laminations is related to the amount of fecal spherulites and the distribution of organic matter. (c) MFT 2: Crumb/vughy microstructure. Made of partially combusted charred plant remains, including charcoal, charred stems, burned coprolites, and other undetermined plant tissue. Sometimes mixed with fresh dung and ash dung patches (PPL). (d) Same as (c) in XPL. (e) MFT 3: Dung ash matrix with fibrous texture that varies from spongy to crumb/vughy microstructure. Abundant darkened spherulites (PPL). (f) Same as (e) in XPL. (g) MFT 4: Plant ash matrix. Common presence of calcified plant material with well-preserved morphology ( $\text{CaCO}_3$  pseudomorphs) (PPL). (h) Same as (g) in XPL. PPL, plain polarized light; XPL, cross-polarized light. [Color figure can be viewed at [wileyonlinelibrary.com](http://wileyonlinelibrary.com)]

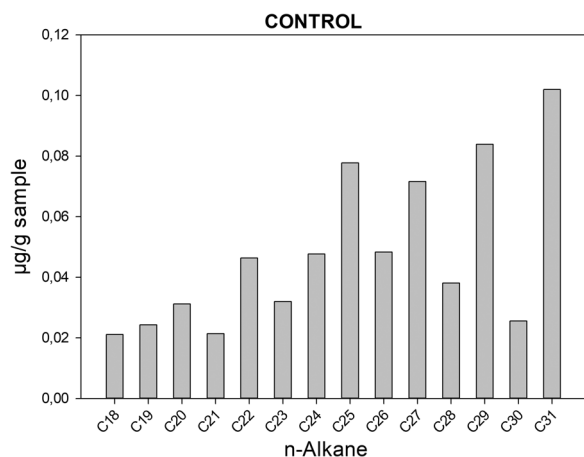


classified into four MFTs according to their micromorphological features, bringing to light a sequence of recurrent depositional events throughout the stratigraphy. Figure 6 shows the distribution of MFTs across Profile A (for Profile B see Supporting Information: Figure S7). Figures 6 and 7 show the main features in each MFT.

### 3.2 | *n*-Alkanes

The modern plant samples show an odd-over-even *n*-alkane predominance, with peak maxima at C<sub>31</sub> and C<sub>33</sub> for *H. hirta*; at C<sub>31</sub> for *B. bituminosa*; at C<sub>27</sub> and C<sub>29</sub> for *E. brevirame*; and at C<sub>27</sub> and C<sub>29</sub> for *L. hillebrandii*.

MFT 1 (unburned dung) samples show an *n*-alkane odd-over-even predominance ranging from C<sub>18</sub> to C<sub>38</sub> (C<sub>max</sub> at C<sub>29</sub>, C<sub>31</sub>, and C<sub>33</sub>) with a total *n*-alkane concentration of 0.10–9.08 µg/gds. Statistical tests, carried out in R version 4.1.1. (R Core Team, 2021), show that the *n*-alkane concentration is significantly higher (analysis of variance [ANOVA],  $F_{2,44} = 5.91$ ,  $p = 0.0053$ ,  $F_{crit} = 3.21$ ) in MFT 1 compared to MFT 2 (carbonized layers) and MFT 3 (dung ash layers) (Supporting Information: Figure S12). MFT 2 samples display total concentration values between 0.00 (detected) and 0.99 µg/gds, ranging from C<sub>18</sub> to C<sub>35</sub>. C<sub>29</sub>, C<sub>31</sub>, and C<sub>33</sub> *n*-alkanes are predominant in an odd-over-even distribution. BM 2-2 displays higher concentrations in the middle chain *n*-alkane (C<sub>23</sub>, C<sub>25</sub>, and C<sub>27</sub>). The total concentration of MFT 3 samples varies between 0.08 and 5.02 µg/gds and their distribution ranges from C<sub>18</sub> to C<sub>35</sub>. C<sub>29</sub>, C<sub>31</sub>, and C<sub>33</sub> dominate again, displaying an odd-over-even predominance in all samples, except for BM 4-2, which shows C<sub>23</sub>, C<sub>25</sub>, and C<sub>27</sub> dominating. BM 7-2, classified as MFT 4 (wood ash), shows a total concentration of 0.00–0.40 µg/gds and a shorter distribution from C<sub>21</sub> to C<sub>35</sub>; again, in an odd-over-even predominance. The control sample shows an odd-over-even predominance ranging from C<sub>24</sub> to C<sub>31</sub> (Figure 8), with C<sub>31</sub> and C<sub>29</sub> as dominating *n*-alkanes.



**FIGURE 8** Control sample histogram showing alkane carbon chain length (x-axis) and their concentrations (µg/gds) (y-axis).

Carbon preference index (CPI), average chain length (ACL), and long-chain alkane ratios have been calculated for each biomarker sample based on concentration (Table 2). CPI values range from 1.31 to 10.93. No statistical differences have been detected between the MFTs (ANOVA,  $F_{2,44} = 0.222$ ,  $p = 0.802$ ,  $F_{crit} = 3.21$ ). ACL mean value is 29.91, showing a prevalence of long-chain alkanes. Normalized long-chain *n*-alkane ratios display a dominance of C<sub>31</sub> and C<sub>33</sub> over C<sub>27</sub> and C<sub>29</sub> across the sequence, except for samples BM 2-2 and BM 4-2 with values > 0.5 (Figure 9). Calculated values and distribution barplots are presented in Supporting Information: Table S2 and Figures S8–S11).

### 3.3 | TC, TIC, and TOC

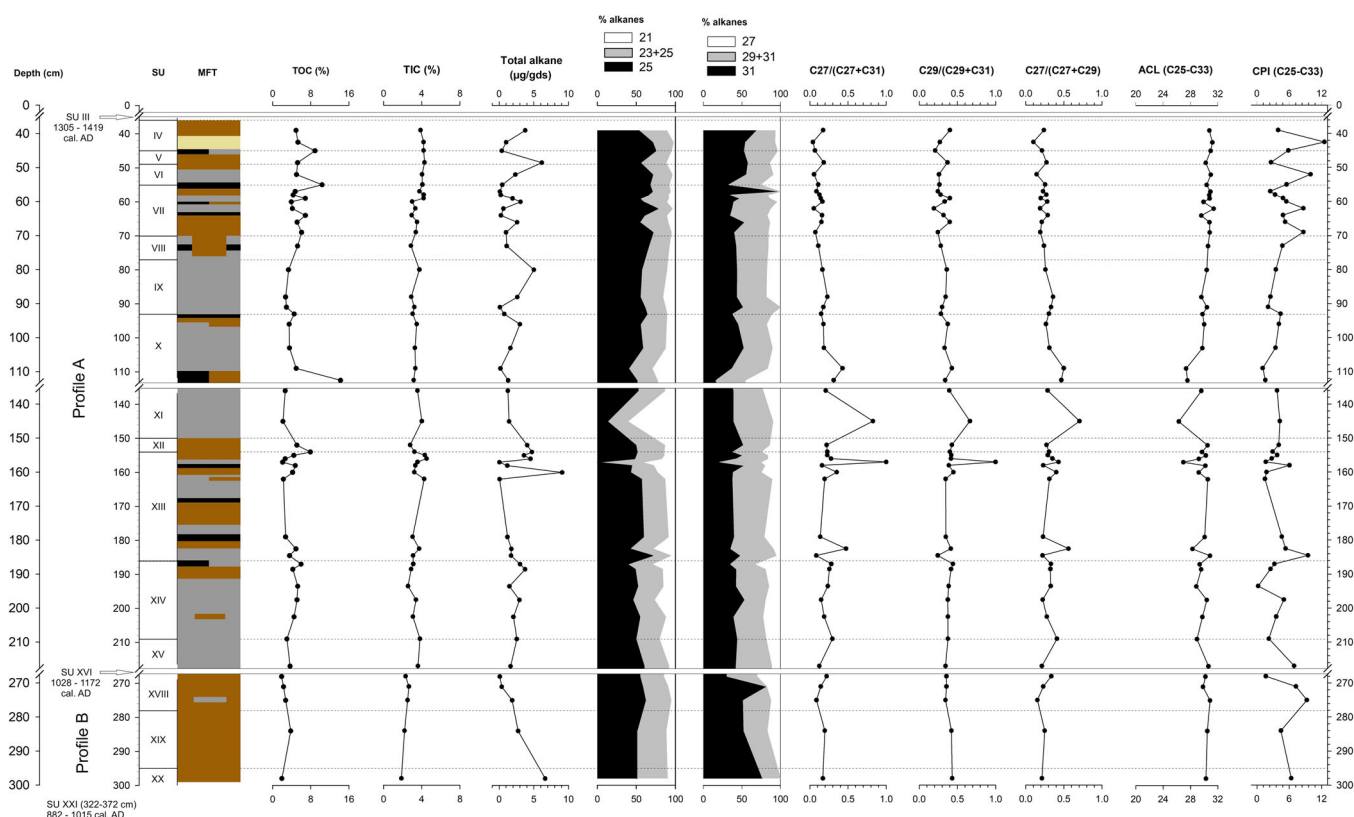
TIC and TOC results are shown in Figure 9. TIC varies from 1.87–4.52% (mean value 3.39%); and TOC ranges from 1.90–14.25% (mean value 4.60%). Statistical analysis shows that MFT 2 (carbonized particles) has significantly higher (ANOVA,  $F_{2,44} = 12.27$ ,  $p = 5.82 \times 10^{-5}$ ,  $F_{crit} = 3.21$ ) TOC values compared to the rest of the MFTs (Supporting Information: Figure S13).

### 3.4 | µ-XRF, µ-XRD, and µ-FTIR

Three types of microanalyses were conducted on the chips that were left over from thin-section production. µ-XRF elemental mapping first targeted areas containing what appeared to be authigenic minerals. A calcium (Ca) µ-XRF elemental map verifies the calcareous matrix of unburned dung layers (filled with calcitic fecal spherulites), dung ash layers, and the plant ash deposit (Figure 10). Ca is also the dominant element present in blades of carbonate formed in the matrix of samples from dung ash layers (Blocks M-01 and M-04). In addition, the distribution of K, P, Mg, and Na closely matches areas of small, numerous crystals, which have previously been defined using optical petrography as authigenic evaporitic crystals (Table 1). An example can be seen in M-01/2, cluster 1 (Figure 11; see also Figure 10 for P distribution). This specific mineral was next analyzed with µ-XRD, also targeting cluster 1, and the resulting pattern showed a match to the mineral hazenite (based on eight reflections) (Figure 12). Finally, µ-FTIR reflectance spectra and diamond ATR spectra were collected from the same cluster (Supporting Information: Figure S14). The resulting spectra showed similarity to reference samples of the mineral struvite, and the reflectance spectrum produced peaks at 1035, 996, and 740 cm<sup>-1</sup> consistent with those reported for hazenite (1040, 990, 750 cm<sup>-1</sup>) by Yang and Sun (2004). Calcium phosphates such as dahllite (1088, 1026, 960, 872, 602, 561 cm<sup>-1</sup>) were also detected through µ-FTIR (Supporting Information: Figure S15, upper). Calcareous needles were also targeted showing both aragonite (874, 853 cm<sup>-1</sup>) and calcite (Supporting Information: Figure S15, lower). Table 3 lists all of the minerals that were identified at the site using a combination of different methods.

TABLE 2 *n*-Alkane ratios.

| Index  | Formula  | References                               |
|--|--|--|
| Carbon preference index (CPI)<br>(C <sub>25</sub> -C <sub>33</sub> ) | $0.5 \times ((C_{25} + C_{27} + C_{29} + C_{31} + C_{33}) / (C_{24} + C_{26} + C_{28} + C_{30} + C_{32}) + (C_{25} + C_{27} + C_{29} + C_{31} + C_{33}) / (C_{26} + C_{28} + C_{30} + C_{32} + C_{34}))$ | Bray and Evans (1961)                    |
| Average chain length (ACL)<br>(C <sub>25</sub> -C <sub>33</sub> )    | $\sum(C_i \times [C_i]) / \sum[C_i]$ ; 25 ≤ <i>i</i> ≤ 33<br>[C <sub><i>i</i></sub> ] = concentration of <i>n</i> -alkane with <i>i</i> carbon atoms   | Cranwell (1973); Poynter et al. (1989)   |
| Normalized long-chain<br><i>n</i> -alkane ratio 1                    | C <sub>27</sub> / (C <sub>27</sub> + C <sub>31</sub> )   | Bai et al. (2009); Schwark et al. (2002) |
| Normalized long-chain<br><i>n</i> -alkane ratio 2                    | C <sub>29</sub> / (C <sub>29</sub> + C <sub>31</sub> )   | Bai et al. (2009); Schwark et al. (2002) |
| Normalized long-chain<br><i>n</i> -alkane ratio 3                    | C <sub>27</sub> / (C <sub>27</sub> + C <sub>29</sub> )   | Bai et al. (2009); Schwark et al. (2002) |



**FIGURE 9** Sedimentary log showing lipid biomarker data across Profiles A and B, from BM 7-1 (uppermost sample) to BM 11-5 (lowermost sample). Colors indicate MFT: brown = MFT 1; black = MFT 2; gray = MFT 3; yellow = MFT 4. Data shown: TOC, TIC, total *n*-alkane concentration, mid-chain *n*-alkane proportions, long-chain *n*-alkane proportions, C<sub>27</sub>/(C<sub>27</sub> + C<sub>31</sub>), C<sub>29</sub>/(C<sub>29</sub> + C<sub>31</sub>), C<sub>27</sub>/(C<sub>27</sub> + C<sub>29</sub>) ratios, ACL, and CPI. ACL, average chain length; CPI, carbon preference index; TIC, total inorganic carbon; TOC, total organic carbon. [Color figure can be viewed at [wileyonlinelibrary.com](http://wileyonlinelibrary.com)]

### 3.5 | Powder XRD and FTIR of loose samples

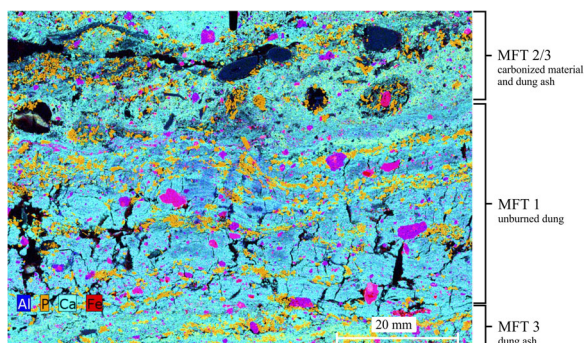
XRD powder analysis was performed on all the MFTs. Calcite (~34%) appeared as the dominant mineral in samples corresponding to unburned dung facies (BM 7-1 and BM 7-4), followed by orthoclase (~18%) sylvite (~9%), hydroxyapatite (no RIR value), and augite (no RIR value). Ash layer BM 4-2 shows a predominance of aragonite (~25%), instead of calcite (~8%), with sylvite also present (~10%)

(Figure 13). Black layer BM 2-2 displays hazenite (~24%), anorthite (~23%), calcite (~14%), sylvite (~13%), microcline (~13%), and hydroxylapatite (~13%).

FTIR analysis of sample BM 4-2 (dung ash) also confirmed the presence of both calcite (1787, 1411, 873, 843, and 712 cm<sup>-1</sup>) and aragonite (1787, 1454, 873, 854, 712 cm<sup>-1</sup>), as well as dahllite (1004, 602, and 565 cm<sup>-1</sup>). BM 7-1 (unburned dung) also shows calcite (1793, 1409, 874, 849, and 712 cm<sup>-1</sup>).

## 4 | DISCUSSION

Micromorphological, elemental, and lipid biomarker data have allowed us to characterize the main formation processes of the Belmaco Cave sedimentary deposit at its central part. The micromorphological data from Profiles A and B show a succession of in situ burnt and unburned goat/sheep dung layers, corroborating the presence of a *fumier* deposit. The

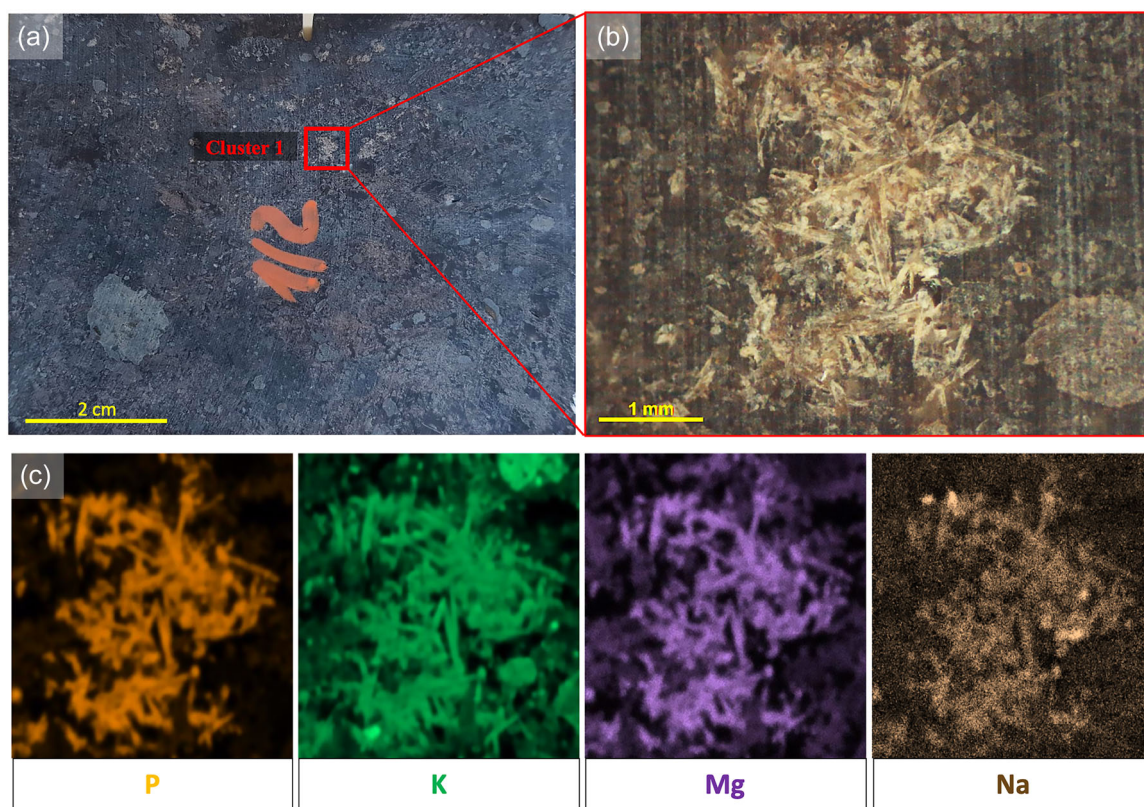


**FIGURE 10** Elemental distribution map of Al, P, Ca, and Fe for sample M-07/2. The map indicates a dominating calcitic matrix. The orange areas correspond to the distribution of hazenite. The image shows the abundance of the mineral in this particular sample. [Color figure can be viewed at [wileyonlinelibrary.com](http://wileyonlinelibrary.com)]

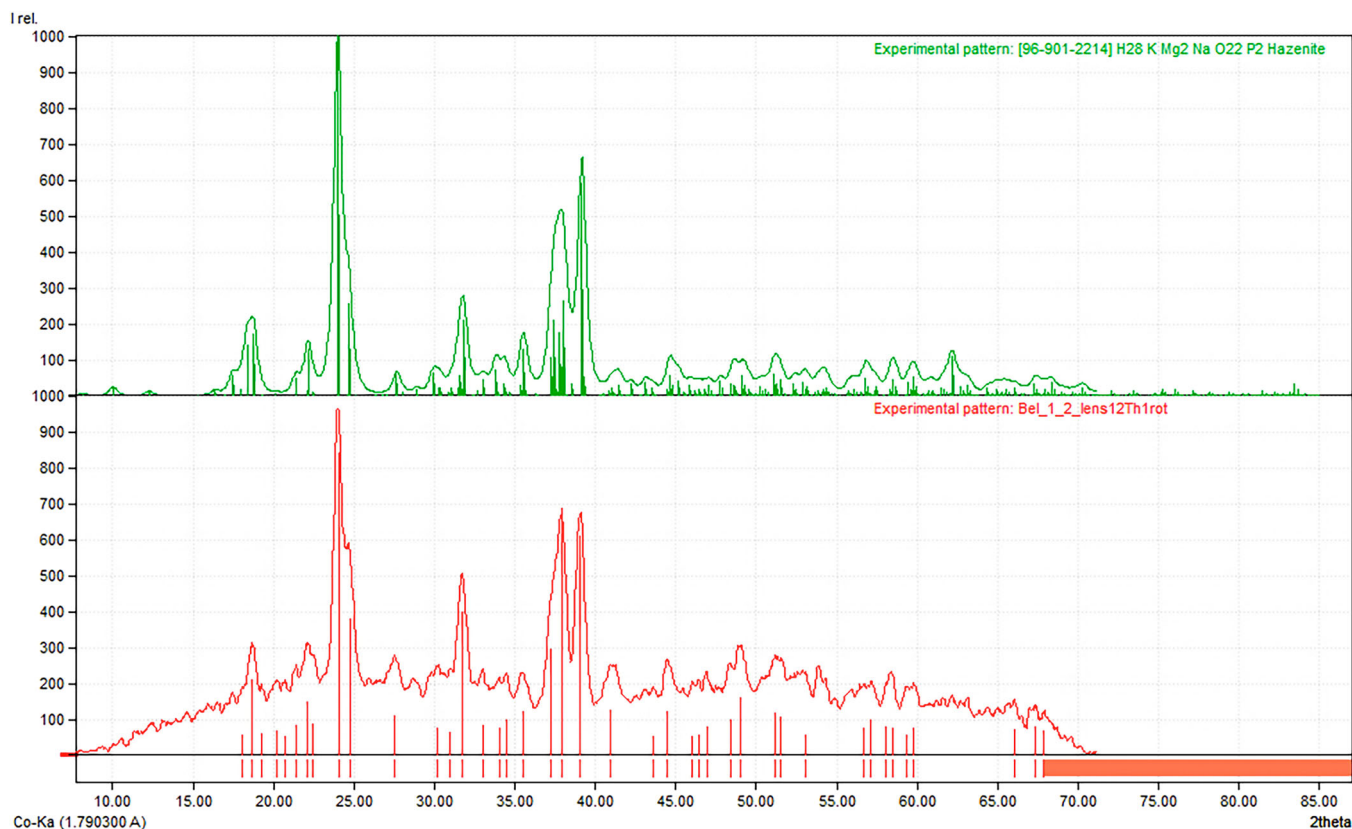
elemental data shows the presence of authigenic salts, carbonates, and phosphates, indicating that this *fumier* deposit is mostly well-preserved, with some secondary mineral formation. *n*-Alkane distribution also points to good preservation of the entire sequence while indicating a predominantly herbaceous plant presence. Thus, the goat/sheep represented by the dung layers possibly had a herb/grass-based diet. Below, we summarize and discuss our main interpretations regarding: (1) the *fumier*'s formation history, (2) diagenesis and other postdepositional processes, and (3) possible plant sources and their preservation. The pattern revealed by our data allows us to formulate a preliminary hypothesis regarding indigenous herding practices in La Palma, which is discussed at the end of this section.

### 4.1 | Formation processes of the *fumier* sequence

The base of the stratigraphic sequence, which corresponds to Profile B (SU XX, XIX, and XVIII), is dominated by an unburned dung matrix (MFT 1) indicative of in situ livestock stabling. No stratified ash layers or spherulitic laminations were observed, except a few thermally altered patches in the uppermost layers (SU XVIII). This basal part is stony and coarse-grained. Illuvial clay coatings of unknown origin are only found in these layers. Therefore, Profile B possibly formed during a period involving stabling events that were not followed by



**FIGURE 11**  $\mu$ -XRF map of crystal cluster identified as hazenite. (a) Chip M-01/2 indicating Cluster 1. (b) Reflected light photograph of hazenite needles in Cluster 1. (c) Elemental composition of Cluster 1, indicating presence of P, K, Mg, and Na.  $\mu$ -XRF,  $\mu$ -X-ray fluorescence. [Color figure can be viewed at [wileyonlinelibrary.com](http://wileyonlinelibrary.com)]



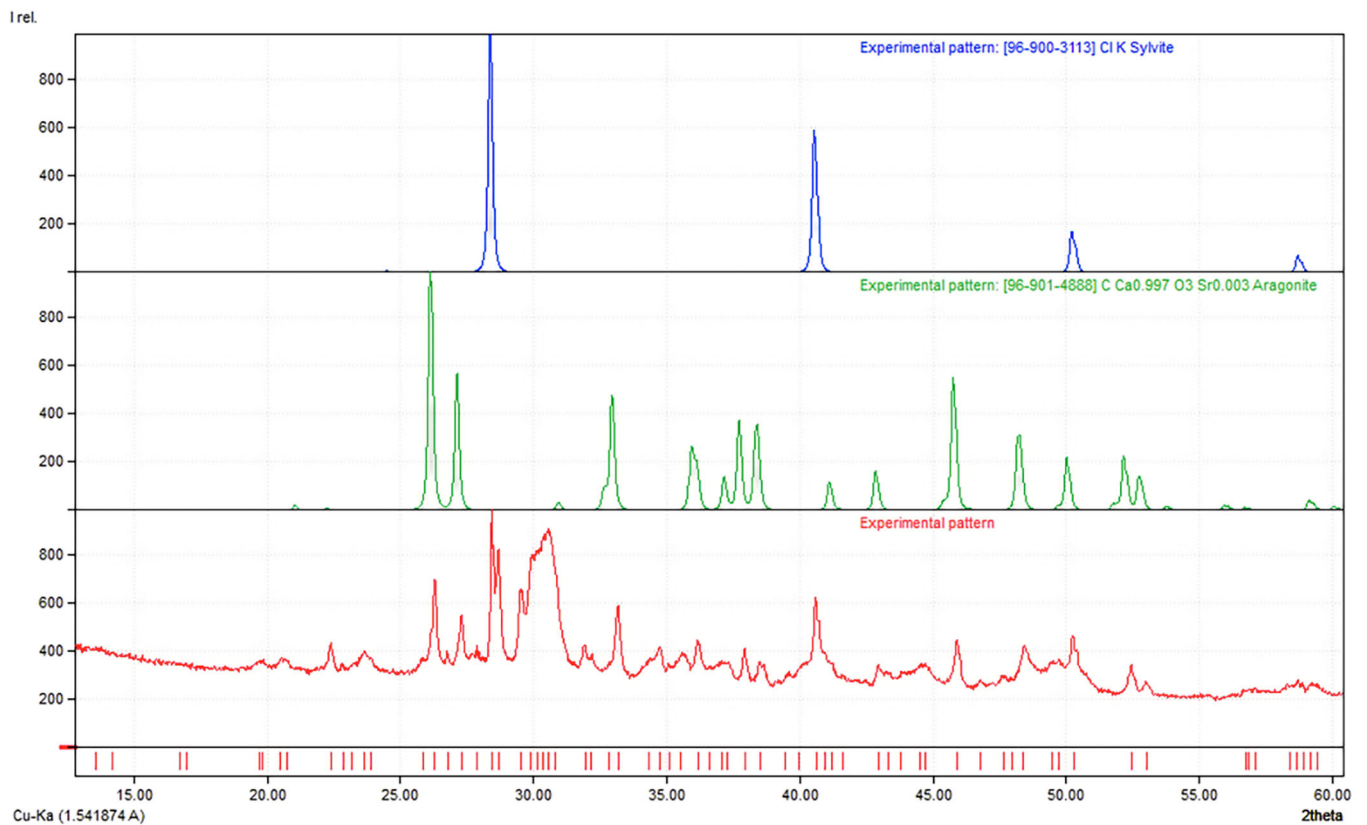
**FIGURE 12**  $\mu$ -XRD on hazenite. Referential pattern (green) is compared to Belmaco pattern (red) from the same sample used in Figure 8 (M-01/2).  $\mu$ -XRD,  $\mu$ -X-ray diffraction. [Color figure can be viewed at [wileyonlinelibrary.com](https://onlinelibrary.wiley.com/doi/10.1002/gea.21972)]

**TABLE 3** Minerals identified in the Belmaco *fumier* deposit.

| Mineral                          | Formula   | Analytical method   | Context  |
|----------------------------------|---|---|--|
| Aragonite                        | CaCO <sub>3</sub>   | Micromorphology, $\mu$ -XRF, FTIR, $\mu$ -FTIR, powder XRD      | Needles in some dung ash layers (MFT 3)  |
| Calcite                          | CaCO <sub>3</sub>   | Micromorphology, $\mu$ -XRF, FTIR, $\mu$ -FTIR                  | Matrix in unburned dung layers (MFT 1), dung ash layers (MFT 3) and wood ash layer (MFT 4)             |
| Dahlite/carbonate hydroxyapatite | Ca <sub>5</sub> (PO <sub>4</sub> , CO <sub>3</sub> ) <sub>3</sub> (OH)  | Micromorphology, powder XRD, $\mu$ -XRF, FTIR, $\mu$ -FTIR      | Nodules in unburned dung layers (MFT 1) and dung ash layers (MFT 3); also present in fragments of bone |
| Anorthite                        | CaAl <sub>2</sub> Si <sub>2</sub> O <sub>8</sub>                        | Powder XRD  | Geogenic fraction; everywhere in the sequence  |
| Microcline                       | KAlSi <sub>3</sub> O <sub>8</sub>                                       | Powder XRD  | Geogenic fraction; everywhere in the sequence  |
| Orthoclase                       | KAlSi <sub>3</sub> O <sub>8</sub>                                       | Powder XRD  | Geogenic fraction; everywhere in the sequence  |
| Sylvite                          | KCl   | Powder XRD, $\mu$ -XRF  | Everywhere in the sequence; possibly concentrated in charcoal (mainly found in MFT 2)                  |
| Hazenite                         | KNaMg <sub>2</sub> (PO <sub>4</sub> ) <sub>2</sub> ·14 H <sub>2</sub> O | Micromorphology, $\mu$ -XRF, powder XRD, micro-XRD, $\mu$ -FTIR | Clusters of crystals everywhere in the sequence  |
| Augite                           | (Ca, Na) (Mg, Fe, Al, Ti) (Si, Al) <sub>2</sub> O <sub>6</sub>          | Micromorphology, powder XRD, $\mu$ -FTIR                        | Geogenic fraction; everywhere in the sequence  |

Note: Does not include amorphous phases, such as the opal present in phytoliths, or volcanic glass.

Abbreviations: FTIR, Fourier-transform infrared spectroscopy;  $\mu$ -XRD,  $\mu$ -X-ray diffraction;  $\mu$ -XRF,  $\mu$ -X-ray fluorescence.



**FIGURE 13** XRD on sylvite and aragonite. Referential patterns of sylvite (blue) and aragonite (green) are compared to the Belmaco pattern (red) from sediment sample BM 4-2 (MFT 3).

intentional burning interspersed with natural geogenic sedimentation comprising a mixed input of gravitational clasts and clayey runoff.

In contrast, Profile A (SU XVII-I), which represents a younger deposit than Profile B, displays a well-bedded, distinctly laminated *fumier* sequence, comprising several stratified MFT sets, which are recurrent throughout the stratified deposit: (1) MFT 1 or mineralized unburned dung layers, which display abundant fecal spherulites and convolute morphologies in the coprolite fragments indicating goat/sheep excrement. These successive stabling events in the cave show compaction, recurrent vertical fissures, and planar voids, possibly as a consequence of animal trampling (Angelucci et al., 2009; Polo-Díaz et al., 2014, 2016); overlain by (2) MFT 2, frequent charcoal, charred plant, and coprolite fragments, possibly representing organic debris lying on the surface of the pen at the time of burning (Égüez et al., 2016; Mallol et al., 2013; Polo-Díaz et al., 2016); and overlain by (3) MFT 3 or dung ashes, which possibly represent dung combustion events related to pastoralist sanitizing practices (Brochier et al., 1992; Macphail et al., 1997; Polo-Díaz, 2010; Vergès et al., 2016) (see Figures 6 and 7). These layers, however, are not laterally continuous across the entire Profile A section, but rather appear to be lenticular, with dimensions varying from half to one meter.

Compared with the unburned dung layers (MFT 1), the ashed dung microfacies (MFT 3) are less compact and contain more frequent plant pseudomorphic voids. This ashed dung layer

represents in situ dung burning. Piling up of waste material to form heaps has been documented as a way of burning dung in southwestern European cave contexts (Polo-Díaz et al., 2016). According to experimental studies, heaps would be distributed across the shelter, functioning as ignition points that help the fire spread across the entire stabling area (Vergès et al., 2016). Sometimes, plant material is laid on top of the piled dung, as a way of adding additional fuel and facilitating the ignition process (Polo-Díaz et al., 2016). Experimental research has also shown that dung does not easily burn on its own and might need plant fuel to achieve ignition depending on the dung moisture content, morphology, and degradation stage (Vergès et al., 2011, 2016). Nevertheless, Shahack-Gross (2011) mentions field observation of spontaneous dung smoldering.

This leads us to MFT 4, which consists of a single wood ash microlayer and entails an exceptional facies compared to the rest of the sampled *fumier* sequence. It is not laterally continuous and overlies a layer of mixed dung and charred plant residues (see Figures 6 and 7). Marrero Salas et al. (2016) documented the presence of possible combustion features across the right section of Profile A (SU III, V, VI, VII, VIII, IX, and XIII), including this wood ash layer in M-07 (Supporting Information: Figure S16). These features could represent the remains of small burning heaps similar to those mentioned earlier. However, macroscopically, they show a smaller size (both in terms of their diameter and stratigraphic depth) than those documented at San Cristóbal rockshelter (Polo-Díaz et al., 2016),



and possibly also than the experimental heaps from Mas del Pepet *fumier* (Vergès et al., 2016). Alternatively, they could represent hearths. Although no micromorphological evidence of domestic activity was observed in the sampled sequence, a few artifacts were recovered from the upper units of Profile A (SU I–IX) in possible stratigraphic association with combustion features (Marrero Salas et al., 2016; Navarro Mederos et al., 2013). Furthermore, archaeological excavations in the northern area, about 8 m away from the *fumier* sequence, brought to light numerous archaeological artifacts and hearths (Diego Cuscoy, 1962). As we move towards the center of the cave (i.e., area covered in this study), the density of archaeological remains decreases. In total, the most recent excavations at the site yielded 160 pottery fragments and 74 lithic artifacts throughout the entire sequence (Marrero Salas et al., 2016; Morales et al., 2007). We only identified one microscopic pottery fragment in sample M-06/1. In light of the current data, Belmaco Cave possibly comprised a domestic space in its northern area and a goat/sheep pen in its south-western area. Similar human–animal cohabitation contexts in rock shelters and caves have been previously reported (Égüez et al., 2016; Karkanas, 2006; Macphail et al., 1997; Polo-Díaz, 2010).

On a few occasions, thin black layers of variable thickness between 0.5 and 3 cm, composed exclusively of charred plants and charcoal (MFT 2) were found between the ashed dung and the unburned compacted dung layers with variably gradational and sharp contacts. Black layers have been documented in other *fumier* contexts, sometimes with similar microstructures and composition to the unburned dung layers, and showing gradational contacts (Angelucci et al., 2009; Bergadà & Oms, 2021; Égüez et al., 2016; Polo-Díaz et al., 2014, 2016). Their reported thickness is around 2–3 cm (Bergadà & Oms, 2021; Égüez et al., 2016). In previous work, they have been interpreted as charred penning surfaces (Égüez et al., 2016; Polo-Díaz et al., 2016), representing the substrate and not the fuel (Mallol et al., 2013). This could also be the case at Belmaco, where black layers show similar thicknesses and structures and directly underlie dung ash, not wood ash. Alternatively, they could represent plant input of unknown origin accumulating on the penning surface during periods of penning inactivity. *Fumier* abandonment periods have been interpreted based on bioturbated facies at Los Husos II (Upper Ebro basin, Spain) (Polo-Díaz, 2010; Polo-Díaz & Fernández Eraso, 2010) and San Cristóbal rock-shelter (Polo-Díaz et al., 2016). In the Belmaco *fumier*, only Block M-06 appears highly bioturbated. Small burrows (~1.5 cm) and occasionally fine coatings surrounding them, with an internal crumb microstructure, seem to indicate termite or ant activity (Mallol & Goldberg, 2017; Marcelino et al., 2010). M-06/2 and M-06/3 middle disturbance seems to have been produced by something bigger than an insect (Supporting Information: Figure S17).

The existing bioturbation at Belmaco is not linked with any particular MFT, in contrast to what Polo-Díaz et al. (2016) report. Due to the marked seasonal contrasts of the region, typical of a dry Mediterranean climate, bioturbation would not be expected for most of the year. In fact, the top layers of the deposit (M-07), affected by subrecent weathering, do not show any signs of soil mesofauna

activity. Our mineralogy data, discussed below, indicate aridity throughout the formation of the deposit, suggesting that environmental conditions have not changed substantially in the last centuries. Instead, slow-degrading surface organic residues at the cave entrance are likely to remain in situ for a relatively long time, which would support the hypothesis that the black layers at Belmaco Cave (MTF 2) could represent periods of penning inactivity.

However, although we did not observe any ash heaps or discrete charcoal-rich combustion structures, our intact black layers are overlain by dung ash layers incorporating scattered combustion residues, which could represent postdepositionally reworked combustion heaps. Moreover, some of the charcoal fragments in the black and dung ash layers are from pinecones and pine needles (see Figure 4d and Supporting Information: Figure S22). These most likely represent *Pinus canariensis*, endemic to the Canarian archipelago and often used as firewood by the indigenous inhabitants (Vidal-Matutano et al., 2021; see their Figure 1 and references therein). In agreement with this evidence, whole charred pinecone scales and pine needles were frequently found in the *fumier* zone during the 1974 and 1979–1980 excavations. Thus, the charred pine residues may represent tinder to facilitate dung burning, with syndepositional and postdepositional disturbance eliminating the ash component and the original combustion structure microstratigraphy. Local shepherds interviewed by JFNM in the 1980s mentioned a tradition of burning a fine layer of pine needles spread across the floors of rockshelter dwellings to eliminate parasites. This tradition persisted in La Palma up to the early 20th century. Altogether, the evidence at hand does not allow us to establish a clear formation process for the black layers at Belmaco Cave, but the most parsimonious interpretation seems to be that they represent residues from anthropogenic plant input including pine, either as fuel or for a different purpose related to the activities carried out in the rockshelter. In any case, a natural source such as wind or gravity is unlikely, as the pine forest is not found in the vicinity of the site.

Interruptions of the penning activity involving deposition of surface organics but *not* subsequently burned by overlying combustion events would be more difficult to identify, except in hyperaridity or waterlogged conditions, as the preservation potential of organic matter (OM) is lower if it is not burnt (Mallol et al., 2013). From this perspective, unburned dung layers (MFT 1), also characterized as brown layers in other contexts, represent a palimpsest of successive penning episodes and their possible abandonment periods, resulting in a homogeneous, brown facies, which has been previously reported in archaeological *fumier* deposits (Bergadà & Oms, 2021; Boschian, 2017; Polo-Díaz et al., 2016).

## 4.2 | Diagenetic processes and secondary mineral formation

Information regarding diagenetic processes at Belmaco Cave has been obtained by combining XRD,  $\mu$ -XRF, FTIR,  $\mu$ -FTIR, and micromorphological data. Mineral phases such as orthoclase,

microcline, and augite are expected in an igneous bedrock context. Calcite and dahllite (carbonated hydroxyapatite) have also been detected through FTIR analyses in *fumier* contexts (Burguet-Coca et al., 2020; Cabanes et al., 2009), and both minerals are common in herbivore dung deposits more generally (Shahack-Gross et al., 2003). Micromorphology shows calcite to be a component of all the MFT, whether it is as fecal spherulites, or component of ash, or recrystallized and authigenic calcite. Three additional minerals were also identified: sylvite, hazenite, and aragonite.

Sylvite (KCl) is present in every sample analyzed using powder XRD. No distinctive corresponding crystalline particles were observed in micromorphological samples, although soluble salts often do not survive the thin-section preparation process, particularly if water is used during sawing. Sylvite has been documented in many cave settings, including several basaltic lava tube caves (Hill & Forti, 1997). In one case, its components are sourced from the basalt itself, with the mineral forming—along with other soluble salts—soon after the formation of the cave while the lava flow cooled in contact with meteoric water (Forti, 2005; Forti et al., 1994). Therefore, one possible internal source of potassium is the dissolution products of the basalt bedrock, as basalt grains visible in thin section show signs of weathering. Another possible internal source is fecal materials and urine. Many examples of sylvite formed in caves are associated with degraded bat guano and urine (Hill & Forti, 1997). A related source that is specific to this type of archaeological site is ruminant urine, as soluble salts have been documented in other archaeological urinerich deposits (Abell et al., 2019). Sylvite in particular has been previously documented in cave pens in Sicily (Brochier et al., 1992). Finally, ashes from some types of plants are known to be rich in soluble forms of potassium (Canti, 2003), and sylvite has been reported as an initial component of wood ashes in experimental replication of campfires by Karkanis (2021). Possible external non-anthropogenic sources of KCl are aerosols and rainfall. Deposition through sea spray is unlikely, as the cave is located at 1.65 km from the coast and reaches an altitude of 362 m a.s.l., which is outside of the range of standard marine aerosol reach (Santos Guerra, 1983). Salt concentration in rainfall is lower than in sea spray (Junge & Werby, 1958), but it could be a potential source of potassium and chlorine. Discriminating which factors are most significant is complex, and a combined contribution of geogenic and biogenic/anthropogenic sources is likely to be the case. To differentiate between the ruminant and geogenic inputs, future sampling should be reoriented outside the *fumier* area within the cave to determine if the presence of sylvite is laterally restricted to areas where animals were kept. Conversely, mineralogical studies of ruminant stabling sedimentary deposits in nonvolcanic settings are key to explore to what extent the parent material plays a role in the formation of evaporites. For example, according to Forti (2005), both volcanic and nonvolcanic caves contain minerals associated with the degradation of guano, but volcanic caves tend to have a wider variety of available ions and therefore a wider range of secondary minerals form. Regarding its preservation at the site, even though sylvite is highly soluble, Belmaco Cave is located in a dry climatic region with long dry

seasons (total rainfall of ca. 544.2 mm/a) (Irl et al., 2015), which may have enhanced the preservation of sylvite. Rain does not usually penetrate into the rockshelter through cracks or joints, and the dripline flow currently falls outward down a slope towards the ravine. Due to its location right below the ceiling line, rain mostly affects Profiles B and C, while Profile A is the least exposed (where sylvite was detected). Alternatively, its presence could be explained as a consequence of lateral migration and precipitation on the Belmaco exposed profiles due to moisture differential (Weiner, 2010).

Authigenic hazenite ( $\text{KNaMg}_2(\text{PO}_4)_2 \cdot 14\text{H}_2\text{O}$ ) was identified through XRD,  $\mu$ -XRD, and  $\mu$ -XRF, and is very abundant in some of the Belmaco sediment samples, with numerous radial clusters of elongated crystals identified in all micromorphological samples (see Figures 5 and 10 for hazenite distribution in M-07/2; Supporting Information: Figure S18 for reflected light photographs; compare to Yang et al., 2011; Figure 1). In thin section, hazenite has angular shapes forming lenticular and tabular euhedral crystals, is colorless in PPL, and displays sky blue to dark blue second-order interference colors in XPL with a parallel extinction.

This is an extremely rare struvite-type phosphate biomineral that has only been documented in a natural setting in Mono Lake (California), which is also located in a volcanic basin (Kelleher & Cameron, 1990). At Mono Lake, the formation of hazenite is related to cyanobacterial *Lyngbya* sp. colonies, and it forms under alkaline conditions in the presence of carbonates (Yang & Sun, 2004; Yang et al., 2011). The identification of hazenite here in Belmaco Cave makes this the second known occurrence of this mineral outside of a laboratory or waste management facility setting. Hazenite has been identified along with other rare members of the struvite group in by-products of fish aquaculture wastewater (Yogev et al., 2020), and in an experimental study of treated human urine exposed to magnesium (Krishnamoorthy et al., 2020). In general, struvite-group minerals are common in human and animal waste, and their formation is a desirable outcome of waste processing, as these minerals are useful for the production of fertilizers.

In archaeological settings, phosphate-containing minerals, in general, are highly representative of decomposing dung deposits and animal husbandry (Holliday & Gartner, 2007; Macphail et al., 2004; Polo-Díaz, 2010; Shahack-Gross, 2011). Struvite-type phosphate minerals, which form in alkaline conditions, have been associated with human urinary stones, decaying OM, urea-rich environments such as stabling floors, and avian or bat guano accumulations in caves (Beck, 1966; Del Moral et al., 1993; Grover et al., 1997; Hill & Forti, 1997). The formation of struvite in the Skipton Lava Cave (Victoria, Australia), for example, is attributed to both the decomposition of bat guano and the weathering of the basalt, which provided a source of magnesium (Bridge, 1971). We speculate that hazenite formed in a similar manner in the Belmaco deposits, with goat/sheep urine and feces probably constituting the main sources for K, P, Na, and some of the Mg (the majority provided by the bedrock), although some contribution from bird guano cannot be excluded. Nowadays, there are bird colonies (*Columba livia*, *Apus*

spp.) inhabiting the cave and accumulating small heaps of guano on the surface (Supporting Information: Figure S19). The presence of avian uric acid in MFT 1 further supports the idea of bird and/or reptile activity around the cave in the past (Supporting Information: Figure S20) (Canti, 1998). Given the strong association of struvite-group minerals, and hazenite in particular, with bacterial activity, we also speculate that bacteria played a role in its formation here. Finally, the presence of both calcite and aragonite in the sediments and presumably alkaline environment aligns with the known formation conditions for hazenite at Mono Lake (Yang et al., 2011). We also note that struvite is unstable in cave settings, and has been observed to alter over time to newberyite and dittmarite (Bridge, 1971; Frost et al., 2011; Snow et al., 2014), so it is possible that the hazenite that we observed may not be the initial or only phosphatic mineral phase present in the cave.

Aragonite, a  $\text{CaCO}_3$  polymorph that commonly crystallizes as needles (Haldar & Tisljar, 2014; Hill & Forti, 1997), was identified through XRD and observed micromorphologically in the SU XI and SU XV dung ash deposits (see Figure 5). In thin section, the aragonite appears as needles/blades with approximate dimensions of  $500 \mu\text{m} \times 50 \mu\text{m}$ , varying in length from 100 to  $1000 \mu\text{m}$ . It displays dark gray absorption colors in PPL, and a high birefringence and high-order green, purple, and white interference colors in XPL. The  $\mu$ -XRF data corroborate a calcitic composition (Supporting Information: Figure S21), while FTIR analysis of loose samples shows the presence of both aragonite and calcite. Biogenic aragonite is usually found in marine organisms (e.g., molluscs and corals). However, Belmaco Cave is not at or near the coast and the sediment does not contain shells from marine organisms or terrestrial land snails. Geogenic formation of aragonite is common in a diversity of cave systems, particularly in evaporitic conditions in the presence of magnesium-rich solutions (Hill & Forti, 1997). Aragonite formation in volcanic settings has been reported as a secondary mineral derived from the dissolution of calcium-rich basalt under high pressure/temperature (Hurai et al., 2013; Yatabe et al., 2000). Another possible source of aragonite is anthropogenic combustion (Toffolo, 2021; Toffolo & Boaretto, 2014; Toffolo et al., 2017). Pyrogenic aragonite has been identified as a small fraction of the calcium carbonate ( $\text{CaCO}_3$ ) that constitutes wood ash (Toffolo & Boaretto, 2014), and is sometimes also documented in burned dung (Dunseth et al., 2019; Gur-Arieh et al., 2014; Weiner, 2010).

Pyrogenic formation could explain the presence of aragonite in our case study. Fecal spherulites and calcium oxalates in plant fragments probably provide the parent material to produce CaO, which is obtained by burning  $\text{CaCO}_3$  above  $600^\circ\text{C}$  (Toffolo & Boaretto, 2014). Considering that aragonite was only documented in the dung ash layers where darkened fecal spherulites have been observed, reaching this temperature seems viable, although we know that temperatures did not exceed  $700^\circ\text{C}$  or no more spherulites would be left (Canti & Nicosia, 2018). Upon recarbonation, the CaO partially turned into aragonite. Since pyrogenic aragonite first forms as needles with lengths of a few hundred nm (Toffolo, 2021), the mm-sized needles observed in the Belmaco samples (see Figure 5c,d)

probably recrystallized over time until reaching that length. Pyrogenic aragonite is very susceptible to dissolution and recrystallization to calcite (Toffolo, 2021), but it is possible that in this setting, the presence of magnesium and the arid climate enhanced the preservation of some of the original mineralogy during the recrystallization process.  $\mu$ -FTIR analysis of the needles indicates that many of them contain a mixture of the two minerals.

The presence of evaporitic minerals in the Belmaco sedimentary sequence is a proxy not only for aridity (pointing to dry conditions throughout its formation) but also for alkalinity. Both aragonite and calcite (e.g., fecal spherulites or ash) are better preserved in alkaline conditions (pH ~8) (Gur-Arieh & Shahack-Gross, 2020; Karkanas, 2016; Toffolo, 2021), aragonite being the least stable of the two carbonate minerals. Given the presence of both  $\text{CaCO}_3$  polymorphs, together with hazenite, we can assume that slight alkaline conditions and available magnesium have dominated at the site until today. On the other hand, the presence of phytoliths in some of the unburned layers suggests that either the pH has not been >8 (Cabanes et al., 2011; Karkanas et al., 2000), or that the moisture levels were low. The most parsimonious explanation for the presence of both alkaline evaporite minerals and phytoliths is that arid conditions were present for most of the time since deposition. This evidence also highlights the potential for good preservation of bone and ash at Belmaco Cave.

In sum, the mineralogy of the archaeosedimentary sequence at Belmaco is consistent with what is expected for a partially burnt dung deposit, as indicated by the presence of  $\text{CaCO}_3$  (calcite and aragonite), and phosphates (dahllite). However, the site also offers what is probably an unusual combination of primary volcanic minerals (e.g., augite, orthoclase, anorthite, and microcline) with halides (e.g., sylvite) and rare phosphates (e.g., hazenite), whose formation might be unique to *fumiers* in arid volcanic settings such as the one presented in this study. The abundance of hazenite, a rare struvite-type phosphate, stands out.

### 4.3 | Organic matter preservation and sources

Our lipid biomarker data address two main aspects of the organic archaeological record: its preservation and its possible sources. The *n*-alkanes generally show good preservation. Their mean concentrations are above  $2 \mu\text{g/gds}$  (see Figure 9) and their distribution displays a strong odd-over-even predominance (Jambrina-Enríquez et al., 2018; Knicker et al., 2013). Black (MFT 2) and dung ash layers (MFT 3) have significantly lower *n*-alkane concentrations compared to the unburned dung layers (MFT 1) (Supporting Information: - Figure S12). Black layers show significantly higher TOC values than unburned dung layers and dung ash layers (Supporting Information: - Figure S13), suggesting higher concentrations and better preservation of other organic compounds (besides *n*-alkanes). This is consistent with experimental studies that have shown that charring and subsequent incomplete combustion around  $300\text{--}350^\circ\text{C}$ , under reduced oxygen conditions, protect OM from microbial degradation

(Braadbaart & Poole, 2008; de la Rosa & Knicker, 2011), while retaining lipid biomarker signatures (Jambrina-Enríquez et al., 2018, 2022; Mallol et al., 2013).

For the dung ash layers (MFT 3), the presence of darkened microscopic dung spherulites suggests burning temperatures of 500–700°C based on published experimental work (Canti & Nicosia, 2018). Rock magnetic studies in *fumiers* also suggest temperatures reaching 600–700°C in ash layers (Burguet-Coca et al., 2022; Carrancho et al., 2012, 2016). However, the *n*-alkane profiles show a strong odd-over-even predominance indicating good preservation (Supporting Information: Figures S10 and S11). This could be related to the existence of patches of charred matter within the ashy facies (see Figure 6, thin sections M-07/2 and M-07/3: charcoal fragments in MFT 3) (Jambrina-Enríquez et al., 2022) or accidental inclusion of sediment from the underlying black layer during the ash layer sampling process.

At Belmaco Cave, CPI values vary throughout the sequence but are consistently higher than 1, meaning an *n*-alkane source of primarily plant origin and a general good preservation of the OM (Bush & McInerney, 2013). The mean CPI value of the *fumier* sequence ( $CPI_{\text{mean}} = 4.5$ ) is higher than the control sample ( $CPI_{\text{control}} = 2.5$ ), because either the *fumier* OM is slightly better preserved or the OM amount is simply greater due to the dung-rich deposit. The range of CPI variability across the *fumier* sequence, from 1.31 to 10.93, does not seem to be linked to the microfacies characteristics themselves (i.e., degradation by thermal alteration). No statistical differences were found (see Section 3) on comparing unburned, carbonized, and ash layers; within each of these, the CPI values differ considerably (see Figure 9). These results require further systematic research and experimental work to identify other factors that might be affecting the degradation indicated by the CPI.

The *n*-alkanes shed some light on possible sources of OM in the Belmaco *fumier* deposit. Our micromorphological observations suggest that the *n*-alkane input is mainly from ruminant excrement, which represents the fodder consumed by sheep/goats. Goat/sheep diet is usually based on dicotyledonous plants and/or grasses (Alonso-Eguiluz et al., 2016; Burguet-Coca et al., 2020; Dunseth et al., 2019; Portillo et al., 2020). The predominance of long-chain *n*-alkanes ( $C_{29}$ ,  $C_{31}$ , and  $C_{33}$ ) across all facies and a mean ACL value of 29.91 are indicative of terrestrial higher plants (herbaceous and woody taxa). All facies are dominated by  $C_{31}$ , which is usually indicative of herbaceous taxa (Cranwell, 1973; Cranwell et al., 1987; Holtvoeth et al., 2016; Meyers, 2003; Zech et al., 2010) or gymnosperms (Diefendorf et al., 2011; Schwark et al., 2002). The control sample ( $C_{\text{max}} = C_{31}$ ) indicates similar *n*-alkane composition in the natural sediment surrounding the site, suggesting the existence of herbaceous vegetation in the natural surroundings.

Given the main composition of the sediments, ruminant dung, the source is more likely to be herbaceous plants than gymnosperms. Peak maxima at  $C_{31}$  have been previously identified in stabling deposits comprising ruminant excrements composed of unburned herbs and grasses (Égüez & Makarewicz, 2018; Égüez et al., 2018). At El Mirador *fumier*, a grass vegetation input in unburned and mixed

burned/unburned layers has been proposed based on the dominance of  $C_{31}$  over  $C_{25}$  and  $C_{27}$  (Vallejo, Gea, Massó, et al., 2022). Furthermore, our preliminary data on La Palma fresh plant material support a dominant herbaceous contribution instead of a woody input. As expected for grasses,  $C_{\text{max}}$  at  $C_{31}$  and  $C_{33}$  dominate in *H. hirta* (native Poaceae). Also, *B. bituminosa* (native Fabaceae) has been characterized as herbaceous (García-Verdugo et al., 2021; Schönfelder & Schönfelder, 2012), which is why  $C_{\text{max}}$  at  $C_{31}$  is compelling. On the other hand, *E. brevirame* (endemic woody shrub; García-Verdugo et al., 2021; Schönfelder & Schönfelder, 2012) was found to have a dominance of  $C_{27}$  and  $C_{29}$  as recorded for woody angiosperms in other regions (Holtvoeth et al., 2016; Meyers, 2003; Zech et al., 2010). The genus *Lotus* in the Canaries represent an insular woodiness adaptation (Jaén-Molina et al., 2021), which probably explains why the *n*-alkane signal in *L. hillebrandii* (endemic Fabaceae) is dominated by  $C_{27}$  and  $C_{29}$ . An input of OM coming from gymnosperms, however, needs to be considered too, given the evidence of pinecones and pine needles in our thin sections (black layer microfacies).

Samples BM 2-2 and BM 4-2 show a different pattern, with dominant mid-chain *n*-alkanes maximizing at  $C_{23}$ . Hygrophilous plants, such as mosses, or aquatic plants, such as emergent or submerged macrophytes, are characterized by *n*-alkane carbon length maxima at  $C_{23}$  and  $C_{25}$  (Ficken et al., 2000; Huang et al., 2010). On the other hand, similar dominant *n*-alkanes have been documented in *Quercus nigra*, *Pinus nigra*, and *Celtis australis* tree wood (Jambrina-Enríquez et al., 2018; Knicker et al., 2013; O'Malley et al., 1997). BM 2-2 is a thick black layer and contains abundant charcoal fragments. Therefore, the *n*-alkane distribution is more likely related to the presence of charcoal as representative of tree branches. Regarding BM 4-2, it is a thick, porous ash layer containing numerous aragonite crystals. Its spongy uncompacted microstructure and primary calcareous composition suggest good preservation and thus dry conditions (Karkanias, 2021), which are further supported by the presence of the relatively soluble mineral aragonite (Toffolo, 2021; Toffolo & Boaretto, 2014). Thus, we discard an *n*-alkane contribution from the presence of hydrophilous vegetation. Instead, the observed predominance of mid-chain alkanes in this sample could also have resulted from the presence of dispersed charcoal in the ash layer, despite being less numerous than BM 2-2. The low representation of microscopically visible charcoal in BM 4-2 highlights the importance of analyses at the molecular scale to identify depositional components that could otherwise go undetected.

#### 4.4 | Indigenous herding practices in La Palma

Pastoralist transhumance in island contexts usually involves seasonal mobility, from summer pastures in the highlands to winter pastures in the lowlands (Elie, 2014; Forgia et al., 2021; MacSween, 1959; Mientjes, 2004). In the Canary Islands, such a pattern exists among contemporary pastoralist communities (Diego Cuscoy, 1968; Navarro Mederos, 1992; Navarro Mederos & Clavijo Redondo, 2001; Pais

Pais, 1996a; Suárez Moreno & Suárez Pérez, 2005). In the eastern islands of Lanzarote and Fuerteventura, which are relatively low and lack vegetation belts, there is also seasonal (summer/winter) horizontal transhumance, which aims to access water supplies and higher-quality pastures (Cabrera Pérez, 1996). In La Palma, contemporary shepherds from the north of the island occupy the lowlands for most of the year and move to the highland pastures of the Taburiente Caldera (~2500 m a.s.l.) in the summer, while in the south, where Belmaco Cave is situated, which has a slightly lower and less rugged terrain, shepherds move back and forth daily, year-round, from the lowlands to the highlands of Cumbre Vieja (~2000 m a.s.l.) (Pais Pais, 1996b). In this study, we have been able to identify a minimum of 10 burnt goat/sheep pen deposits formed in a time interval of 150–400 years represented in Profile A, which could reflect either snapshots of a seasonal mobility pattern (with a few random abandonment periods preserved by combustion and the rest concealed by the palimpsest effect) or several centuries of year-round goat/sheep penning at the cave with daily pasturing in the highlands,—similar to contemporary southern shepherds in La Palma, interrupted by a minimum of 10 abandonment periods involving burning of the pen surface. If we consider that the mean retention time of food in goat/sheep digestive tract is around 48 h (Tsiplakou et al., 2011), and consider a scenario in which indigenous shepherds practiced similar daily mobilities as modern ones, transiting from the lowlands to the highlands of Cumbre Vieja and back within the same day, the fecal matter that is being deposited at Belmaco should retain vegetation markers from the summit, midlands, and coastal areas. Our *n*-alkane data, dominated by a herbaceous signal, still cannot discriminate between herbs and grasses from the highlands versus those from the lowlands. Thus, the C<sub>31</sub> dominance could potentially come from human-introduced ruderal nitrophilous flora, abundantly found along contemporary pastoral routes (e.g., *Chenopodium* spp., *Amaranthus* spp., *Malva* spp., *Fumaria* spp., *Solanum nigrum*, *Trifolium* sp., *Plantago* spp., *Conyza* spp.) (del Arco Aguilar et al., 2010; Morales et al., 2007), or from nonruderal endemic or nonendemic native herb and grass species found in the ecosystems transited by modern shepherds and documented as commonly-used fodder: coastal shrubland (*Cenchrus ciliaris*, *Wahlenbergia lobelioides*, *Forsskaolea angustifolia*, *Aristida adscensionis*), thermophile woodlands (*H. hirta*, *Asphodelus* spp., *Urginea* spp.), *Erica-Morella* woody heath (*Brachypodium sylvaticum*, *Gallium scabrum*, *Origanum vulgare*, *Drusa glandulosa*), and Canarian pine forest (*L. hillebrandii*, *Cicer canariensis*, *Ornithopus compressus*, *Tuberaria guttata*) (del Arco Aguilar, 2006; Pais Pais, 1996a; Pérez de Paz et al., 1994; Santos Guerra, 1983).

Significantly, the presence of pine elements, such as pine needles, discovered at Belmaco, adds to the growing body of evidence documenting the use of external fuel sources at indigenous sites in the Canary Islands (Machado Yanes & Ourcival, 1998; Machado Yanes, 1999; Tomé et al., 2022; Vidal-Matutano et al., 2019). Currently, pine formations can be found approximately 3 km away from Belmaco Cave, at an altitude difference of 600 m. According to del Arco Aguilar (2006), the potential distribution of the pine forest, uninfluenced by human activities, is not significantly

different from its present distribution. While there is a lack of paleoecological and paleoclimatic data regarding vegetation distribution before human arrival and during prehistoric times in La Palma, it is plausible to consider a scenario in which indigenous herders residing in Belmaco Cave would journey to higher elevations, where the pine forest exists today at over 1000 m a.s.l., to gather specific types of fuel and possibly exploit the rich understory as fodder. This is in agreement with ecological research suggesting that the understory of the present-day La Palma pine forest has been depleted due to centuries of anthropogenic overgrazing (Garzón-Machado et al., 2010; Irl et al., 2014).

Further investigations are necessary to test the different hypotheses: (1) archaeological work in *fumier* contexts from the north of the island will allow us to explore pastoralist mobility strategies in a different orographic setting; (2) analysis of compound-specific carbon stable isotopes on *n*-alkanes to assess differences in summit versus coast vegetation; (3) extension of our preliminary reference leaf wax *n*-alkane data from native and endemic plants of La Palma to corroborate the plant sources of the Belmaco Cave *fumier* deposit; (4) phytolith analysis to complement the biomolecular data and further assess herd dietary patterns and preservation.

## 5 | CONCLUDING REMARKS

Microcontextual data gathered at the central area of Belmaco Cave have brought to light the existence of a late indigenous *fumier* deposit. The use of the cave as a pen for livestock dates from 9th to the 15th century A.D. Similar to other animal enclosures in cave contexts, the pen was periodically burned to sanitize the space and ensure its reutilization over the centuries, a practice that had not been reported in the Canarian indigenous literature from a high-resolution geoarchaeological perspective. A minimum of ten burning episodes were identified across the 600–1100-year-old sequence. The OM present in the sedimentary deposit, primarily derived from goat/sheep excrements, is well preserved, under generally dry and charred conditions, as shown by the geochemical and mineralogical data, and its lipid molecular residues represent higher plants, possibly herbaceous taxa. This study provides a new multiproxy, geoarchaeological framework for the investigation of *fumier* sedimentary deposits aimed at reconstructing formation processes and plant fodder sources to approach pastoralist herding practices.

## AUTHOR CONTRIBUTIONS

**Enrique Fernández-Palacios:** Conceptualization; investigation; writing—original draft; formal analysis; visualization. **Margarita Jambriña-Enríquez:** Conceptualization; supervision; writing—original draft. **Susan M. Mentzer:** Investigation; writing—original draft; resources; visualization. **Caterina Rodríguez de Vera:** Investigation; writing—review and editing. **Ada Dinckal:** Investigation; writing—review and editing; visualization. **Natalia Égüez:** Visualization; writing—review and editing. **Antonio V. Herrera-Herrera:** Writing—review and editing; formal analysis. **Juan Francisco Navarro Mederos:** Resources;

writing—review and editing. **Efraín Marrero Salas**: Resources; writing—review and editing. **Christopher E. Miller**: Conceptualization; supervision; resources; writing—review and editing. **Carolina Mallol**: Conceptualization; funding acquisition; project administration; supervision; resources; writing—original draft.

## ACKNOWLEDGMENTS


We thank Cristo M. Hernández Gómez and the members of the PRORED Soc. Coop. for their fieldwork. We are also grateful to Thomas Beckmann for thin-section manufacture, the lab personnel at IPE-SCIC for Total Organic and Inorganic Carbon analyses, and the lab personnel at Servicio Integrado de Difracción de Rayos X (SIDIX, SEGAI, University of La Laguna) for X-ray diffraction analysis. We also thank Michael Toffolo, Katleen Deckers, David Brönnimann, Matthew G. Canti, and Alvaro Castilla-Beltrán for their comments and suggestions during this research, and Laura Tomé for her help in the artwork. We finally thank the anonymous reviewers for their helpful comments and suggestions. This research was funded by the Fundación Caja Canarias and “La Caixa” (Project 2018PATRI19) and the FPU predoctoral contract awarded to EFP (FPU19/02379) by the Spanish Ministry of Universities. We thank the Cabildo Insular de La Palma and Jorge Pais Pais for supporting this research and providing permits.

## CONFLICT OF INTEREST STATEMENT

The authors declare no conflict of interest.

## ORCID

Enrique Fernández-Palacios  <http://orcid.org/0000-0002-3055-0009>

Margarita Jambina-Enríquez  <http://orcid.org/0000-0001-7545-9164>

Susan M. Mentzer  <http://orcid.org/0000-0002-3117-8448>

Caterina Rodríguez de Vera  <http://orcid.org/0000-0002-9750-2052>

Ada Dinckal  <http://orcid.org/0000-0001-6570-7793>

Natalia Égüez  <http://orcid.org/0000-0001-8853-8064>

Antonio V. Herrera-Herrera  <http://orcid.org/0000-0002-4313-766X>

Juan Francisco Navarro Mederos  <http://orcid.org/0000-0002-2293-8513>

Efraín Marrero Salas  <http://orcid.org/0000-0003-2547-0095>

Carolina Mallol  <http://orcid.org/0000-0001-5143-4253>

## REFERENCES

- Abell, J. T., Quade, J., Duru, G., Mentzer, S. M., Stiner, M. C., Uzdurum, M., & Özbaşaran, M. (2019). Urine salts elucidate early neolithic animal management at Aşıklı Höyük, Turkey. *Science Advances*, 5, eaaw0038. <https://doi.org/10.1126/sciadv.aaw0038>
- Abreu, J. (1977). In A. Cioranescu (Ed.), *Historia de la Conquista de las Siete Islas de Canaria*. Goya ediciones, Santa Cruz de Tenerife.
- Allué, E., Vernet, J.-L., & Cebrià, A. (2009). Holocene vegetational landscapes of NE Iberia: Charcoal analysis from Cova de la Guineu, Barcelona, Spain. *The Holocene*, 19(5), 765–773. <https://doi.org/10.1177/0959683609105301>
- Alonso-Eguiluz, M. (2012). Estudio de los fitolitos en conjuntos de la Prehistoria reciente en la Sierra de Cantabria. El caso de los niveles de redil de San Cristóbal (Laguadía, Álava). *Estudios de Cuaternario/Kuaternario Ikasketak/Quaternary Studies (CKQ)*, 2, 1–14.
- Alonso-Eguiluz, M., Fernández-Eraso, J., & Albert, R. M. (2016). The first herders in the upper Ebro basin at Los Husos II (Álava, Spain): Microarchaeology applied to fumier deposits. *Vegetation History and Archaeobotany*, 26, 143–157. <https://doi.org/10.1007/s00334-016-0590-y>
- Angelucci, D. E., Boschian, G., Fontanals, M., Pedrotti, A., & Vergès, J. M. (2009). Shepherds and karst: The use of caves and rock-shelters in the Mediterranean region during the Neolithic. *World Archaeology*, 41, 191–214. <https://doi.org/10.1080/00438240902843659>
- Bai, Y., Fang, X., Nie, J., Wang, Y., & Wu, F. (2009). A preliminary reconstruction of the paleoecological and paleoclimatic history of the Chinese Loess Plateau from the application of biomarkers. *Palaeogeography, Palaeoclimatology, Palaeoecology*, 271(1), 161–169. <https://doi.org/10.1016/j.palaeo.2008.10.006>
- Beck, C. W. (1966). Apatitic urinary calculi from early American Indians. *JAMA: The Journal of the American Medical Association*, 195, 1044–1045.
- Bergadà, M. M., & Oms, F. X. (2021). Pastoral practices, bedding and fodder during the early neolithic through micromorphology at Cova Colomera (Southeastern Pre-Pyrenees, Iberia). *Open Archaeology*, 7, 1258–1273. <https://doi.org/10.1515/opar-2020-0183>
- Boschian, G. (2017). Pastoral sites. In A. S. Gilbert (Ed.), *Encyclopedia of Geoarchaeology* (pp. 644–651). Springer.
- Braadbaart, F., & Poole, I. (2008). Morphological, chemical and physical changes during charcoalification of wood and its relevance to archaeological contexts. *Journal of Archaeological Science*, 35, 2434–2445. <https://doi.org/10.1016/j.jas.2008.03.016>
- Bray, E. E., & Evans, E. D. (1961). Distribution of n-paraffins as a clue to recognition of source beds. *Geochimica et Cosmochimica Acta*, 22(1), 2–15. [https://doi.org/10.1016/0016-7037\(61\)90069-2](https://doi.org/10.1016/0016-7037(61)90069-2)
- Bridge, P. J. (1971). Analyses of altered struvite from Skipton, Victoria. *Mineralogical Magazine*, 38, 381–382.
- Brochier, J. E. (1983a). Bergeries et feux de bois néolithiques dans le Midi de la France: caractérisation et incidence sur le raisonnement sédimentologique. *Quartär*, 33–34, 119–135.
- Brochier, J. E. (1983b). Combustion et parage des herbivores domestiques. Le point de vue du sédimentologue. *Bulletin de la Société Préhistorique Française*, 80, 143–145.
- Brochier, J. E. (1991). Géoaarchéologie du monde agropastoral. In J. Guilaine (Ed.), *Pour une archéologie agraire A* (pp. 303–322). Colin. Paris.
- Brochier, J. E. (1996). Feuillies ou fumiers? Observations sur le rôle des poussières sphérolitiques dans l'interprétation des dépôts archéologiques holocènes. *Anthropozoologica*, 24, 19–30.
- Brochier, J. E. (2002). Les sédiments anthropiques: méthodes d'étude et perspectives. In J. C. Miskovswy (Ed.), *Géologie de la Préhistoire: méthodes, techniques, applications, Geopré* (pp. 453–477). Perpignan.
- Brochier, J. E., Villa, P., Giacomarra, M., & Tagliacozzo, A. (1992). Shepherds and sediments: Geo-ethnoarchaeology of pastoral sites. *Journal of Anthropological Archaeology*, 11, 47–102. [https://doi.org/10.1016/0278-4165\(92\)90010-9](https://doi.org/10.1016/0278-4165(92)90010-9)
- Burguet-Coca, A., Polo-Díaz, A., Martínez-Moreno, J., Benito-Calvo, A., Allué, E., Mora, R., & Cabanes, D. (2020). Pen management and livestock activities based on phytoliths, dung spherulites, and minerals from Cova Gran de Santa Linya (Southeastern pre-Pyrenees). *Archaeological and Anthropological Sciences*, 12, 148. <https://doi.org/10.1007/s12520-020-01101-6>
- Burguet-Coca, A., Del Valle, H., Expósito, I., Herrejón-Lagunilla, Á., Buitkute, E., Cabanes, D., Cáceres, I., Carrancho, Á., & Villalain, J. J.

- (2022). The Fumier sequences of El Mirador: An approach to fire as a sociocultural practice and taphonomic agent. In E. Allué, P. Martín, & J. M. Vergès (Eds.), *Prehistoric herders and farmers: A transdisciplinary overview to the Archeological record from El Mirador Cave* (pp. 89–110). Springer International Publishing. [https://doi.org/10.1007/978-3-031-12278-1\\_5](https://doi.org/10.1007/978-3-031-12278-1_5)
- Bush, R. T., & McInerney, F. A. (2013). Leaf wax n-alkane distributions in and across modern plants: Implications for paleoecology and chemotaxonomy. *Geochimica et Cosmochimica Acta*, 117, 161–179. <https://doi.org/10.1016/j.gca.2013.04.016>
- Cabanes, D., Weiner, S., & Shahack-Gross, R. (2011). Stability of phytoliths in the archaeological record: a dissolution study of modern and fossil phytoliths. *Journal of Archaeological Science*, 38, 2480–2490. <https://doi.org/10.1016/j.jas.2011.05.020>
- Cabanes, D., Burjachs, F., Expósito, I., Rodríguez, A., Allué, E., Euba, I., & Vergès, J. M. (2009). Formation processes through archaeobotanical remains: The case of the bronze age levels in El Mirador cave, Sierra de Atapuerca, Spain. *Quaternary International*, 193, 160–173. <https://doi.org/10.1016/j.quaint.2007.08.002>
- Cabrera Pérez, J. C. (1996). *La Prehistoria de Fuerteventura: un modelo insular de adaptación*. Servicio de Publicaciones del Cabildo Insular de Fuerteventura, Ediciones del Cabildo Insular de Gran Canaria, Las Palmas de Gran Canaria.
- Canti, M. G. (1998). The micromorphological identification of faecal spherulites from archaeological and modern materials. *Journal of Archaeological Science*, 25, 435–444.
- Canti, M. G. (2003). Aspects of the chemical and microscopic characteristics of plant ashes found in archaeological soils. *Catena*, 54, 339–361. [https://doi.org/10.1016/S0341-8162\(03\)00127-9](https://doi.org/10.1016/S0341-8162(03)00127-9)
- Canti, M. G., & Nicosia, C. (2018). Formation, morphology and interpretation of darkened faecal spherulites. *Journal of Archaeological Science*, 89, 32–45. <https://doi.org/10.1016/j.jas.2017.11.004>
- Carracedo, J. C., Rodríguez Badiola, E., & Guillou, H. (2015). Mapa geológico y Memoria de la Hoja nº 1085 III/IV (Isla de La Palma/El Pueblo). Mapa Geológico de España, Escala: 1/25.000. Instituto Geológico y Minero de España.
- Carrancho, Á., Herrejón Lagunilla, Á., & Vergès, J. M. (2016). Three archaeomagnetic applications of archaeological interest to the study of burnt anthropogenic cave sediments. *Quaternary International*, 414, 244–257. <https://doi.org/10.1016/j.quaint.2015.10.010>
- Carrancho, Á., Villalain, J. J., Vergès, J. M., & Vallverdú, J. (2012). Assessing post-depositional processes in archaeological cave fires through the analysis of archaeomagnetic vectors. *Quaternary International*, 275, 14–22. <https://doi.org/10.1016/j.quaint.2012.01.010>
- Chung, F. H. (1974). Quantitative interpretation of X-ray diffraction patterns of mixtures. I. Matrix-flushing method for quantitative multicomponent analysis. *Journal of Applied Crystallography*, 7, 519–525.
- Cioranescu, A. (2004). *Crónicas francesas de la conquista de Canarias. Le Canarien*. Idea, Santa Cruz de Tenerife.
- Connolly, R., Jambriña-Enríquez, M., Herrera-Herrera, A. V., Vidal-Matutano, P., Fagoaga, A., Marquina-Blasco, R., Marin-Monfort, M. D., Ruiz-Sánchez, F. J., Laplana, C., Bailon, S., Pérez, L., Leierer, L., Hernández, C. M., Galván, B., & Mallol, C. (2019). A multiproxy record of palaeoenvironmental conditions at the Middle Palaeolithic site of Abric del Pastor (Eastern Iberia). *Quaternary Science Reviews*, 225, 106023. <https://doi.org/10.1016/j.quascirev.2019.106023>
- Courty, M. A. (2001). Microfacies analysis assisting archaeological stratigraphy. In P. Goldberg, V. T. Holliday, & C. R. Ferring (Eds.), *Earth sciences and archaeology* (pp. 205–239). Springer. [https://doi.org/10.1007/978-1-4615-1183-0\\_8](https://doi.org/10.1007/978-1-4615-1183-0_8)
- Cranwell, P. A. (1973). Chain-length distribution of n-alkanes from lake sediments in relation to post-glacial environmental change. *Freshwater Biology*, 3, 259–265. <https://doi.org/10.1111/j.1365-2427.1973.tb00921.x>
- Cranwell, P. A., Eglinton, G., & Robinson, N. (1987). Lipids of aquatic organisms as potential contributors to lacustrine sediments—II. *Organic Geochemistry*, 11, 513–527. [https://doi.org/10.1016/0146-6380\(87\)90007-6](https://doi.org/10.1016/0146-6380(87)90007-6)
- de la Rosa, J. M., & Knicker, H. (2011). Bioavailability of N released from N-rich pyrogenic organic matter: An incubation study. *Soil Biology and Biochemistry*, 43, 2368–2373. <https://doi.org/10.1016/j.soilbio.2011.08.008>
- de Nascimento, L., Willis, K. J., Fernández-Palacios, J. M., Criado, C., & Whittaker, R. J. (2009). The long-term ecology of the lost forests of La Laguna, Tenerife (Canary Islands). *Journal of Biogeography*, 36, 499–514. <https://doi.org/10.1111/j.1365-2699.2008.02012.x>
- de Nascimento, L., Nogué, S., Criado, C., Ravazzi, C., Whittaker, R. J., Willis, K. J., & Fernández-Palacios, J. M. (2016). Reconstructing Holocene vegetation on the island of Gran Canaria before and after human colonization. *The Holocene*, 26, 113–125. <https://doi.org/10.1177/0959683615596836>
- de Nascimento, L., Nogué, S., Naranjo-Cigala, A., Criado, C., McGlone, M., Fernández-Palacios, E., & Fernández-Palacios, J. M. (2020). Human impact and ecological changes during prehistoric settlement on the Canary Islands. *Quaternary Science Reviews*, 239, 106332. <https://doi.org/10.1016/j.quascirev.2020.106332>
- del Arco, C. (1993). *Recursos vegetales en la prehistoria de Canarias*. Museo Arqueológico, Cabildo de Tenerife.
- del Arco Aguilar, M. J. (Ed.). (2006). *Mapa de vegetación de Canarias*. GRAFCAN ediciones, Santa Cruz de Tenerife.
- del Arco Aguilar, M. J., González-González, R., Garzón-Machado, V., & Pizarro-Hernández, B. (2010). Actual and potential natural vegetation on the Canary Islands and its conservation status. *Biodiversity and Conservation*, 19, 3089–3140. <https://doi.org/10.1007/s10531-010-9881-2>
- Del Moral, A., Roldan, E., Rivadeneyra, M. A., Monteoliva-Sanchez, M., Perez-García, I., & Ramos-Cormenzana, A. (1993). Formation of struvite crystals by bacteria from human urine and renal calculi. *Biomedical Letters*, 48, 287–290.
- Delhon, C., Martin, L., & Thiébaud, S. (2023). Neolithic shepherds and sheepfold caves in Southern France and adjacent areas: An overview from 40 years of bioarchaeological analyses. *Quaternary International*, in press. <https://doi.org/10.1016/j.quaint.2023.03.004>
- Delhon, C., Martin, L., Argant, J., & Thiébaud, S. (2008). Shepherds and plants in the Alps: Multi-proxy archaeobotanical analysis of neolithic dung from “La Grande Rivoire” (Isère, France). *Journal of Archaeological Science*, 35(11), 2937–2952. <https://doi.org/10.1016/j.jas.2008.06.007>
- Diefendorf, A. F., Freeman, K. H., Wing, S. L., & Graham, H. V. (2011). Production of n-alkyl lipids in living plants and implications for the geologic past. *Geochimica et Cosmochimica Acta*, 75, 7472–7485. <https://doi.org/10.1016/j.gca.2011.09.028>
- Diego Cuscoy, L. (1962). *Memoria de las excavaciones en Belmaco*. Museo Arqueológico del Puerto de la Cruz, Puerto de la Cruz.
- Diego Cuscoy, L. (1968). *Los guanches. Vida y cultura del primitivo habitante de Tenerife*. Museo Arqueológico de Tenerife, Santa Cruz de Tenerife.
- Dove, H., & Mayes, R. W. (1996). Plant wax components: A new approach to estimating intake and diet composition in herbivores. *The Journal of Nutrition*, 126, 13–26. <https://doi.org/10.1093/jn/126.1.13>
- Dove, H., & Mayes, R. W. (2005). Using n-alkanes and other plant wax components to estimate intake, digestibility and diet composition of grazing/browsing sheep and goats. *Small Ruminant Research*, 59, 123–139. <https://doi.org/10.1016/j.smallrumres.2005.05.016>
- Dunseth, Z. C., Fuks, D., Langgut, D., Weiss, E., Melamed, Y., Butler, D. H., Yan, X., Boaretto, E., Tepper, Y., Bar-Oz, G., & Shahack-Gross, R. (2019). Archaeobotanical proxies and archaeological interpretation: A comparative study of phytoliths, pollen and seeds in dung pellets

- and refuse deposits at Early Islamic Shivta, Negev, Israel. *Quaternary Science Reviews*, 211, 166–185. <https://doi.org/10.1016/j.quascirev.2019.03.010>
- Eglinton, G., & Hamilton, R. J. (1967). Leaf epicuticular waxes. *Science*, 156, 1322–1335. <https://doi.org/10.1126/science.156.3780.1322>
- Égüez, N., & Makarewicz, C. A. (2018). Carbon isotope ratios of plant n-alkanes and microstratigraphy analyses of dung accumulations in a pastoral nomadic winter campsite (Eastern Mongolia). *Ethnoarchaeology*, 10, 141–158. <https://doi.org/10.1080/19442890.2018.1510614>
- Égüez, N., Zerbóni, A., & Biagetti, S. (2018). Microstratigraphic analysis on a modern central Saharan pastoral campsite. Ovicaprines pellets and stabling floors as ethnographic and archaeological referential data. *Quaternary International*, 483, 180–193. <https://doi.org/10.1016/j.quaint.2017.12.016>
- Égüez, N., Mallol, C., & Makarewicz, C. A. (2022). n-Alkanes and their carbon isotopes ( $\delta^{13}C$ ) reveal seasonal foddering and long-term corralling of pastoralist livestock in eastern Mongolia. *Journal of Archaeological Science*, 147, 105666. <https://doi.org/10.1016/j.jas.2022.105666>
- Égüez, N., Mallol, C., Martín-Socas, D., & Camalich, M. D. (2016). Radiometric dates and micromorphological evidence for synchronous domestic activity and sheep penning in a Neolithic cave: Cueva de El Toro (Málaga, Antequera, Spain). *Archaeological and Anthropological Sciences*, 8, 107–123. <https://doi.org/10.1007/s12520-014-0217-0>
- Elie, S. D. (2014). Pastoralism in Soqatra: External entanglements and communal mutations. *Pastoralism*, 4, 16. <https://doi.org/10.1186/s13570-014-0016-3>
- Euba, I., Allué, E., & Burjachs, F. (2016). Wood uses at El Mirador Cave (Atapuerca, Burgos) based on anthracology and dendrology. *Quaternary International*, 414, 285–293. <https://doi.org/10.1016/j.quaint.2015.08.084>
- Expósito, I., & Burjachs, F. (2016). Taphonomic approach to the palynological record of burnt and unburnt samples from El Mirador Cave (Sierra de Atapuerca, Burgos, Spain). *Quaternary International*, 414, 258–271. <https://doi.org/10.1016/j.quaint.2016.01.051>
- Fernández Eraso, J., & Polo Díaz, A. (2009). Establos en abrigos bajo roca de la Prehistoria Reciente: su formación, caracterización y proceso de estudio. *Los casos de Los Husos y de San Cristóbal*. *Krei*, 10, 39–51.
- Fernández-Palacios, J. M., Nogué, S., Criado, C., Connor, S., Góis-Marques, C., Sequeira, M., & de Nascimento, L. (2016). Climate change and human impact in Macaronesia. *Past Global Change Magazine*, 24, 68–69. <https://doi.org/10.22498/pages.24.2.68>
- Ficken, K. J., Li, B., Swain, D. L., & Eglinton, G. (2000). An n-alkane proxy for the sedimentary input of submerged/floating freshwater aquatic macrophytes. *Organic Geochemistry*, 31, 745–749. [https://doi.org/10.1016/S0146-6380\(00\)00081-4](https://doi.org/10.1016/S0146-6380(00)00081-4)
- Forgia, V., Ollé, A., & Vergès, J. M. (2021). Early pastoral communities in the mountains of Sicily. Prehistoric evidence from Vallone Inferno (Scillato) in the palaeoenvironmental framework of the Madonie mountain range. *Journal of Anthropological Archaeology*, 61, 101238. <https://doi.org/10.1016/j.jaa.2020.101238>
- Forti, P. (2005). Genetic processes of cave minerals in volcanic environments: An overview. *Journal of Cave and Karst Studies*, 67, 3–13.
- Forti, P., Giudice, G., Marino, A., & Rossi, A. (1994). La Grotta Cutrona (MC1) sul Monte Etna e i suoi speleotemi metastabili. *Atti Congresso Regionale Di Speleologia, Catania*, 125–151.
- Fregel, R., Pestano, J., Arnay, M., Cabrera, V. M., Larruga, J. M., & González, A. M. (2009). The maternal aborigine colonization of La Palma (Canary Islands). *European Journal of Human Genetics*, 17, 1314–1324. <https://doi.org/10.1038/ejhg.2009.46>
- Frost, R. L., Palmer, S. J., & Pogson, R. E. (2011). Raman spectroscopy of newberyite Mg (PO<sub>3</sub>OH)·3H<sub>2</sub>O: A cave mineral. *Spectrochimica Acta, Part A: Molecular and Biomolecular Spectroscopy*, 79, 1149–1153.
- García-Verdugo, C., Mairal, M., Tamaki, I., & Msanda, F. (2021). Phylogeography at the crossroad: Pleistocene range expansion throughout the Mediterranean and back-colonization from the Canary Islands in the legume *Bituminaria bituminosa*. *Journal of Biogeography*, 48, 1622–1634. <https://doi.org/10.1111/jbi.14100>
- Garzón-Machado, V., González-Mancebo, J. M., Palomares-Martínez, A., Acevedo-Rodríguez, A., Fernández-Palacios, J. M., del Arco-Aguilar, M., & Pérez-de-Paz, P. L. (2010). Strong negative effect of alien herbivores on endemic legumes of the Canary pine forest. *Biological Conservation*, 143, 2685–2694. <https://doi.org/10.1016/j.biocon.2010.07.012>
- Gea, J., Sampedro, M. C., Vallejo, A., Polo-Díaz, A., Goicolea, M. A., Fernández-Eraso, J., & Barrio, R. J. (2017). Characterization of ancient lipids in prehistoric organic residues: Chemical evidence of livestock-pens in rock-shelters since early Neolithic to bronze age. *Journal of Separation Science*, 40, 4549–4562. <https://doi.org/10.1002/jssc.201700692>
- Grover, J. E., Rope, A. F., & Kaneshiro, E. S. (1997). The occurrence of biogenic calcian struvite, (Mg, Ca) NH<sub>4</sub> PO<sub>4</sub>·6H<sub>2</sub>O, as intracellular crystals in paramecium. *The Journal of Eukaryotic Microbiology*, 44, 366–373. <https://doi.org/10.1111/j.1550-7408.1997.tb05679.x>
- Gur-Arieh, S., & Shahack-Gross, R. (2020). Ash and dung calcitic microremains. In A. G. Henry (Ed.), *Handbook for the analysis of micro-particles in archaeological samples* (pp. 117–147). Springer. [https://doi.org/10.1007/978-3-030-42622-4\\_6](https://doi.org/10.1007/978-3-030-42622-4_6)
- Gur-Arieh, S., Shahack-Gross, R., Maeir, A. M., Lehmann, G., Hitchcock, L. A., & Boaretto, E. (2014). The taphonomy and preservation of wood and dung ashes found in archaeological cooking installations: Case studies from Iron Age Israel. *Journal of Archaeological Science*, 46, 50–67. <https://doi.org/10.1016/j.jas.2014.03.011>
- Haldar, S. K., & Tisljar, J. (2014). *Introduction to mineralogy and petrology*. Elsevier.
- Hernández Pérez, M. (1999). *La cueva de Belmaco (Mazo-Isla de La Palma)* (Vol. 7). Dirección General de Patrimonio Histórico, Santa Cruz de Tenerife.
- Herrera-Herrera, A. V., & Mallol, C. (2018). Quantification of lipid biomarkers in sedimentary contexts: Comparing different calibration methods. *Organic Geochemistry*, 125, 152–160. <https://doi.org/10.1016/j.orggeochem.2018.07.009>
- Hill, C., & Forti, P. (1997). *Cave minerals of the world*. National Speleological Society.
- Holliday, V. T., & Gartner, W. G. (2007). Methods of soil P analysis in archaeology. *Journal of Archaeological Science*, 34, 301–333. <https://doi.org/10.1016/j.jas.2006.05.004>
- Holtvoeth, J., Rushworth, D., Copsey, H., Imeri, A., Cara, M., Vogel, H., Wagner, T., & Wolff, G. A. (2016). Improved end-member characterisation of modern organic matter pools in the Ohrid Basin (Albania, Macedonia) and evaluation of new palaeoenvironmental proxies. *Biogeosciences*, 13, 795–816. <https://doi.org/10.5194/bg-13-795-2016>
- Huang, X., Wang, C., Xue, J., Meyers, P. A., Zhang, Z., Tan, K., Zhang, Z., & Xie, S. (2010). Occurrence of diplotene in moss species from the Dajihu Peatland in Southern China. *Organic Geochemistry*, 41, 321–324. <https://doi.org/10.1016/j.orggeochem.2009.09.008>
- Hurai, V., Huraiova, M., Milovsky, R., Luptakova, J., & Konecny, P. (2013). High-pressure aragonite phenocrysts in carbonatite and carbonated syenite xenoliths within an alkali basalt. *American Mineralogist*, 98, 1074–1077. <https://doi.org/10.2138/am.2013.4410>
- Irl, S. D. H., Steinbauer, M. J., Messinger, J., Blume-Werry, G., Palomares-Martínez, Á., Beierkuhnlein, C., & Jentsch, A. (2014). Burned and



- devoured—Introduced herbivores, fire, and the endemic flora of the high-elevation ecosystem on La Palma, Canary Islands. *Arctic, Antarctic and Alpine Research*, 46, 859–869. <https://doi.org/10.1657/1938-4246-46.4.1>
- Irl, S. D. H., Harter, D. E. V., Steinbauer, M. J., Gallego Puyol, D., Fernández-Palacios, J. M., Jentsch, A., & Beierkuhnlein, C. (2015). Climate vs. topography—Spatial patterns of plant species diversity and endemism on a high-elevation island. *Journal of Ecology*, 103, 1621–1633. <https://doi.org/10.1111/1365-2745.12463>
- Jaén-Molina, R., Marrero-Rodríguez, Á., Caujapé-Castells, J., & Ojeda, D. I. (2021). Molecular phylogenetics of Lotus (Leguminosae) with emphasis in the tempo and patterns of colonization in the Macaronesian region. *Molecular Phylogenetics and Evolution*, 154, 106970. <https://doi.org/10.1016/j.ympev.2020.106970>
- Jambrina-Enríquez, M., Herrera-Herrera, A. V., & Mallol, C. (2018). Wax lipids in fresh and charred anatomical parts of the *Celtis australis* tree: Insights on paleofire interpretation. *Organic Geochemistry*, 122, 147–160. <https://doi.org/10.1016/j.orggeochem.2018.05.017>
- Jambrina-Enríquez, M., Mallol, C., Tostevin, G., Monnier, G., Pajović, G., Borovinić, N., & Baković, M. (2022). Hydroclimate reconstruction through MIS 3 in the Middle Paleolithic site of Crvena Stijena (Montenegro) based on hydrogen-isotopic composition of sedimentary n-alkanes. *Quaternary Science Reviews*, 295, 107771. <https://doi.org/10.1016/j.quascirev.2022.107771>
- Junge, C. E., & Werby, R. T. (1958). The concentration of chloride, sodium, potassium, calcium, and sulfate in rainwater over the United States. *Journal of Meteorology*, 15, 417–425. [https://doi.org/10.1175/1520-0469\(1958\)015<0417:TCOCSP>2.0.CO;2](https://doi.org/10.1175/1520-0469(1958)015<0417:TCOCSP>2.0.CO;2)
- Karkanas, P. (2006). Late Neolithic household activities in marginal areas: The micromorphological evidence from the Kouveleiki caves, Peloponnese, Greece. *Journal of Archaeological Science*, 33, 1628–1641.
- Karkanas, P. (2016). Chemical alteration. In S. A. Gilbert (Ed.), *Encyclopedia of geoarchaeology* (pp. 129–138). Springer.
- Karkanas, P. (2021). All about wood ash: Long-term fire experiments reveal unknown aspects of the formation and preservation of ash with critical implications on the emergence and use of fire in the past. *Journal of Archaeological Science*, 135, 105476. <https://doi.org/10.1016/j.jas.2021.105476>
- Karkanas, P., Bar-Yosef, O., Goldberg, P., & Weiner, S. (2000). Diagenesis in Prehistoric Caves: The use of minerals that form in situ to assess the completeness of the archaeological record. *Journal of Archaeological Science*, 27, 915–929. <https://doi.org/10.1006/jasc.1999.0506>
- Kelleher, P. C., & Cameron, K. L. (1990). The geochemistry of the mono craters-mono lake islands volcanic complex, eastern California. *Journal of Geophysical Research*, 95, 17643. <https://doi.org/10.1029/jb095ib11p17643>
- Knicker, H., Hilscher, A., de la Rosa, J. M., González-Pérez, J. A., & González-Vila, F. J. (2013). Modification of biomarkers in pyrogenic organic matter during the initial phase of charcoal biodegradation in soils. *Geoderma*, 197–198, 43–50. <https://doi.org/10.1016/j.geoderma.2012.12.021>
- Krishnamoorthy, N., Dey, B., Arunachalam, T., & Paramasivan, B. (2020). Effect of storage on physicochemical characteristics of urine for phosphate and ammonium recovery as struvite. *International Biodeterioration & Biodegradation*, 153, 105053. <https://doi.org/10.1016/j.ibiod.2020.105053>
- Lafuente, B., Downs, R. T., Yang, H., & Stone, N. (2016). The power of databases: The RRUFF project. In T. Armbruster & R. M. Danisi (Eds.), *Highlights in mineralogical crystallography* (pp. 1–29). De Gruyter.
- Lancelotti, C., Balbo, A. L., Madella, M., Iriarte, E., Rojo-Guerra, M., Royo, J. I., Tejedor, C., Garrido, R., García, I., Arcusa, H., Pérez Jordà, G., & Peña-Chocarro, L. (2014). The missing crop: Investigating the use of grasses at Els Trocs, a Neolithic cave site in the Pyrenees (1564 m asl). *Journal of Archaeological Science*, 42, 456–466. <https://doi.org/10.1016/j.jas.2013.11.021>
- Leierer, L., Jambrina-Enríquez, M., Herrera-Herrera, A. V., Connolly, R., Hernández, C. M., Galván, B., & Mallol, C. (2019). Insights into the timing, intensity and natural setting of Neanderthal occupation from the geoarchaeological study of combustion structures: A micromorphological and biomarker investigation of El Salt, unit Xb, Alcoy, Spain. *PLoS One*, 14, e0214955. <https://doi.org/10.1371/journal.pone.0214955>
- Machado Yanes, M. C. (1999). El hombre y las transformaciones del medio vegetal en el Archipiélago Canario durante el período pre-europeo-500 a. C./1500 d. C. *Sanguntum Plau, Extra 2*, 53–58.
- Machado Yanes, M. C., & Ourcival, J. M. (1998). La evolución de la vegetación del Norte de Tenerife durante el periodo prehistórico. *Arqueología espacial*, 19–20, 249–260.
- Macphail, R., Courty, M. A., Hather, J., & Watte, J. (1997). The soil micromorphological evidence of domestic occupation and stabling activities. In R. Maggi (Ed.), *Arene Candide: A functional and environmental assessment of the Holocene sequence (excavations Bernabò Brea-Cardini 1940–50)* (pp. 53–88). Memorie dell'Istituto Italiano di Paleontologia Umana.
- Macphail, R. I., Cruise, G. M., Allen, M. J., Linderholm, J., & Reynolds, P. (2004). Archaeological soil and pollen analysis of experimental floor deposits; with special reference to Butser Ancient Farm, Hampshire, UK. *Journal of Archaeological Science*, 31, 175–191. <https://doi.org/10.1016/j.jas.2003.07.005>
- MacSween, M. D. (1959). Transhumance in North Skye. *Scottish Geographical Magazine*, 75, 75–88. <https://doi.org/10.1080/00369225908735747>
- Mallol, C., & Goldberg, P. (2017). Cave and rock shelter sediments. In C. Nicosia & G. Stoops (Eds.), *Archaeological soil and sediment micromorphology* (pp. 357–382). John Wiley & Sons.
- Mallol, C., Hernández, C. M., Cabanes, D., Sistiaga, A., Machado, J., Rodríguez, Á., Pérez, L., & Galván, B. (2013). The black layer of Middle Palaeolithic combustion structures. Interpretation and archaeostratigraphic implications. *Journal of Archaeological Science*, 40, 2515–2537. <https://doi.org/10.1016/j.jas.2012.09.017>
- Marcelino, V., Stoops, G., & Schaefer, C. E. G. R. (2010). Oxidic and related materials. In G. Stoops, V. Marcelino, & F. Mees (Eds.), *Interpretation of micromorphological features of soils and regoliths* (pp. 305–327). Elsevier.
- Marrero Salas, E., Navarro Mederos, J. F., García Ávila, J. C., Abreu Hernández, I., Pou Hernández, S., & Álvarez Rodríguez, N. (2016). La alternancia ocupacional en la cueva de Belmaco, La Palma. Una revisión arqueosedimentaria. *XXI Coloquio de Historia Canario-Americana* (2014), XXI-071, 1–19. <http://coloquioscanariamerica.casadecolon.com/index.php/aea/article/view/9554>
- Martín Rodríguez, E. (1992). *La Palma y los auaritas*. Centro de la Cultura Popular Canaria, Santa Cruz de Tenerife.
- Mentzer, S. M. (2016). Rockshelter settings. In A. S. Gilbert (Ed.), *Encyclopedia of geoarchaeology* (pp. 725–743). Springer.
- Meyers, P. A. (2003). Applications of organic geochemistry to paleolimnological reconstructions: A summary of examples from the Laurentian Great Lakes. *Organic Geochemistry*, 34, 261–289. [https://doi.org/10.1016/S0146-6380\(02\)00168-7](https://doi.org/10.1016/S0146-6380(02)00168-7)
- Mientjes, A. C. (2004). Modern pastoral landscapes on the island of Sardinia (Italy). Recent pastoral practices in local versus macro-economic and macro-political contexts. *Archaeological Dialogues*, 10, 161–190. <https://doi.org/10.1017/S1380203804001230>
- Morales, J. (2003). *De textos y semillas. Una aproximación etnobotánica a la prehistoria de Canarias*. El Museo Canario, Las Palmas de Gran Canaria.

- Morales, J., & Gil, J. (2014). Gathering in a New Environment: The Use of Wild Food Plants during the First Colonization of the Canary Islands, Spain (2nd–3rd century BCE to 15th century CE). In A. Chevalier, E. Marinova, & L. Peña-Chocarro (Eds.), *An offprint from plants and people: Choices and diversity through time* (pp. 216–264). Oxbow Books.
- Morales, J., Alberto Barroso, V., & Rodríguez Rodríguez, A. (2007). Intervención arqueológica en el yacimiento de Belmaco (campaña del año 2000). Nuevas aportaciones al estudio de macrorrestos vegetales en la isla de La Palma. *Revista de Estudios Generales de La Isla de La Palma*, 3, 135–160.
- Morales, J., Rodríguez-Rodríguez, A., & Marrero, Á. (2014). Prehistoric plant use on La Palma island (Canary Islands, Spain). An example of the disappearance of agriculture in an isolated environment. In C. J. Stevens, S. Nixon, M. A. Murray, & D. Q. Fuller (Eds.), *Archaeology of African plant use* (pp. 195–204). Left Coast Press.
- Morales, J., Rodríguez Rodríguez, A., & Henríquez-Valido, P. (2017). Agricultura y recolección vegetal en la arqueología prehistórica de las Islas Canarias (siglos III–XV d.C.): la contribución de los estudios carpológicos. In J. Fernández Eraso, J. A. Mujika Alustiza, Á. Arrizabalaga Valbuena, M. García Díez, & L. Zapata Peña (Eds.), *Miscelánea en homenaje a Lydia Zapata Peña* (pp. 189–218). Universidad del País Vasco, Bilbao.
- Morales, J., Rodríguez, A., Alberto, V., Machado, C., & Criado, C. (2009). The impact of human activities on the natural environment of the Canary Islands (Spain) during the pre-Hispanic stage (3rd–2nd century BC to 15th century AD): An overview. *Environmental Archaeology*, 14, 27–36. <https://doi.org/10.1179/174963109X400655>
- Navarro Mederos, J. F. (1992) *Los gomeros. Una prehistoria insular*. Dirección General de Patrimonio Histórico, Gobierno de Canarias, Santa Cruz de Tenerife.
- Navarro Mederos, J. F., & Clavijo Redondo, M. A. (2001). La comisaría de excavaciones arqueológicas en las Canarias occidentales: sobre el balance y trascendencia de Luis Diego Cuscoy. *Faykag. Revista Canaria de Arqueología*, 2–18. <http://faykag.cjb.net>
- Nicosia, C., & Stoops, G. (Eds.). (2017). *Archaeological soil and sediment micromorphology*. John Wiley & Sons. <https://doi.org/10.1002/9781118941065>
- Navarro Mederos, J. F., Marrero Salas, E., García Ávila, J. C., & Abreu Hernández, I. (2013). Memoria de Intervención de Urgencia en el Caboco de Belmaco (Villa de Mazo, isla de La Palma). Universidad de La Laguna.
- O'Malley, V. P., Burke, R. A., & Schlotzhauer, W. S. (1997). Using GC–MS/Combustion/IRMS to determine the  $^{13}\text{C}/^{12}\text{C}$  ratios of individual hydrocarbons produced from the combustion of biomass materials—Application to biomass burning. *Organic Geochemistry*, 27, 567–581. [https://doi.org/10.1016/S0146-6380\(97\)00087-9](https://doi.org/10.1016/S0146-6380(97)00087-9)
- Pais Pais, F. J. (1996a). *La economía de producción en la prehistoria de la isla de La Palma: la ganadería*. Dirección General de Patrimonio Histórico, Viceconsejería de Cultura y Deportes, Gobierno de Canarias. Santa Cruz de Tenerife.
- Pais Pais, F. J. (1996b). Los asentamientos pastoriles prehistóricos del reborde montañoso que contornea la caldera de Taburiente. *Tabona: Revista de Prehistoria y de Arqueología*, 9, 149–164.
- Pais Pais, F. J. (2008). Estrategias sociales en la explotación del territorio entre los benahoaritas. *Actas del VI Congreso de Patrimonio Histórico (Lanzarote)*, 1–30.
- Pais Pais, F. J. (2017). *Belmaco*. Le Canarien ediciones, Excmo. Ayuntamiento de la Villa de Mazo, Mazo.
- Pérez de Paz, P. L., del Arco Aguilar, M. J., Rodríguez Delgado, O., Acebes Ginovés, J. R., Marrero Gómez, M. V., & Wildpret de la Torre, W. (1994). *Atlas cartográfico de los pinares canarios III. La Palma*. Viceconsejería de Media Ambiente. Gobierno de Canarias. Santa Cruz de Tenerife.
- Pescini, V., Carbonell, A., Colominas, L., Égüez, N., Mayoral, A., & Palet, J. M. (2023). Neolithic livestock practices in high mountain areas: A multi-proxy study of pastoral enclosures of Molleres II (Eastern Pyrenees). *Quaternary International*, in press. <https://doi.org/10.1016/j.quaint.2023.04.008>
- Peters, K. E., Walters, C. C., & Moldovan, J. M. (2007). *The biomarker guide: Volume 1. Biomarkers and isotopes in the environment and human history*. Cambridge University Press. <https://doi.org/10.1017/CBO9780511524868>
- Polo Díaz, A., & Fernández Eraso, J. (2010). Same anthropogenic activity, different taphonomic processes: A comparison of deposits from Los Husos I & II (Upper Ebro Basin, Spain). *Quaternary International*, 214, 82–97. <https://doi.org/10.1016/j.quaint.2009.10.022>
- Polo-Díaz, A. (2010). *Rediles prehistóricos y uso del espacio en abrigos bajo roca en la Cuenca Alta del Ebro: Geoarqueología y procesos de formación durante el Holoceno*. Universidad del País Vasco.
- Polo-Díaz, A., Martínez-Moreno, J., Benito-Calvo, A., & Mora, R. (2014). Prehistoric herding facilities: Site formation processes and archaeological dynamics in Cova Gran de Santa Linya (Southeastern Prepyrenees, Iberia). *Journal of Archaeological Science*, 41, 784–800. <https://doi.org/10.1016/j.jas.2013.09.013>
- Polo-Díaz, A., Alonso-Eguíluz, M., Ruiz, M., Pérez, S., Mújika, J., Albert, R. M., & Fernández Eraso, J. (2016). Management of residues and natural resources at San Cristóbal rock-shelter: Contribution to the characterisation of chalcolithic agropastoral groups in the Iberian Peninsula. *Quaternary International*, 414, 202–225. <https://doi.org/10.1016/j.quaint.2016.02.013>
- Portillo, M., García-Suárez, A., & Matthews, W. (2020). Livestock faecal indicators for animal management, penning, foddering and dung use in early agricultural built environments in the Konya Plain, Central Anatolia. *Archaeological and Anthropological Sciences*, 12, 40. <https://doi.org/10.1007/s12520-019-00988-0>
- Poynter, J. G., Farrimond, P., Robinson, N., & Eglinton, G. (1989). Aeolian-derived higher plant lipids in the marine sedimentary record: Links with palaeoclimate. In M. Leinen, & M. Sarnthein (Eds.), *Paleoclimatology and Paleometeorology: Modern and past patterns of global atmospheric transport* (pp. 435–462). Springer. [https://doi.org/10.1007/978-94-009-0995-3\\_18](https://doi.org/10.1007/978-94-009-0995-3_18)
- R Core Team. (2021). *R: A language and environment for statistical computing*. R Foundation for Statistical Computing. <https://www.R-project.org/>
- Ravazzi, C., Mariani, M., Criado, C., Garozzo, L., Naranjo-Cigala, A., Perez-Torrado, F. J., Pini, R., Rodriguez-Gonzalez, A., Nogué, S., Whittaker, R. J., Fernández-Palacios, J. M., & Nascimento, L. (2021). The influence of natural fire and cultural practices on island ecosystems: Insights from a 4,800-year record from Gran Canaria, Canary Islands. *Journal of Biogeography*, 48, 276–290. <https://doi.org/10.1111/jbi.13995>
- Rodríguez, A., Allué, E., & Buxó, R. (2016). Agriculture and livestock economy among prehistoric herders based on plant macro-remains from El Mirador (Atapuerca, Burgos). *Quaternary International*, 414, 272–284. <https://doi.org/10.1016/j.quaint.2016.01.045>
- Santos Guerra, A. (1983). *Vegetación y flora de La Palma*. Interinsular Canaria, Santa Cruz de Tenerife.
- Schönfelder, P., & Schönfelder, I. (2012). *Die Kosmos-Kanarenflora*. Kosmos.
- Schwark, L., Zink, K., & Lechterbeck, J. (2002). Reconstruction of postglacial to early Holocene vegetation history in terrestrial Central Europe via cuticular lipid biomarkers and pollen records from lake sediments. *Geology*, 30, 463–466. [https://doi.org/10.1130/00917613\(2002\)030<0463:ROPTEH>2.0.CO;2](https://doi.org/10.1130/00917613(2002)030<0463:ROPTEH>2.0.CO;2)
- Shahack-Gross, R. (2011). Herbivorous livestock dung: Formation, taphonomy, methods for identification, and archaeological significance. *Journal of Archaeological Science*, 38, 205–218. <https://doi.org/10.1016/j.jas.2010.09.019>

- Shahack-Gross, R., Marshall, F., & Weiner, S. (2003). Geo-Ethnoarchaeology of pastoral sites: The identification of livestock enclosures in abandoned Maasai settlements. *Journal of Archaeological Science*, 30, 439–459. <https://doi.org/10.1006/jasc.2002.0853>
- Snow, M. R., Pring, A., & Allen, N. (2014). Minerals of the Wooltana Cave, Flinders Ranges, South Australia. *Transactions of the Royal Society of South Australia*, 138, 214–230.
- Stoops, G. (2021). *Guidelines for analysis and description of soil and regolith thin sections* (2nd ed.). John Wiley & Sons.
- Stoops, G., Marcelino, V. & Mees, F. (Eds.). (2018). *Interpretation of micromorphological features of soils and regoliths*. Elsevier. <https://doi.org/10.1016/c2014-0-01728-5>
- Suárez Moreno, F., & Suárez Pérez, A. (2005). *Guía del Patrimonio Etnográfico de Gran Canaria*. Cabildo Insular de Gran Canaria, Las Palmas de Gran Canaria.
- The Helen and Martin Kimmel Center for Archaeological Science Infrared Spectra Library. (2022, April, 6). <https://centers.weizmann.ac.il/kimmel-arch/infrared-spectra-library>
- Toffolo, M. B. (2021). The significance of aragonite in the interpretation of the microscopic archaeological record. *Geoarchaeology*, 36, 149–169. <https://doi.org/10.1002/gea.21816>
- Toffolo, M. B., & Boaretto, E. (2014). Nucleation of aragonite upon carbonation of calcium oxide and calcium hydroxide at ambient temperatures and pressures: A new indicator of fire-related human activities. *Journal of Archaeological Science*, 49, 237–248. <https://doi.org/10.1016/j.jas.2014.05.020>
- Toffolo, M. B., Regev, L., Mintz, E., Poduska, K. M., Shahack-Gross, R., Berthold, C., Miller, C. E., & Boaretto, E. (2017). Accurate radiocarbon dating of archaeological ash using pyrogenic aragonite. *Radiocarbon*, 59, 231–249. <https://doi.org/10.1017/RDC.2017.7>
- Tomé, L., Jambriña-Enríquez, M., Égüez, N., Herrera-Herrera, A. V., Davara, J., Marrero Salas, E., Arnay de la Rosa, M., & Mallol, C. (2022). Fuel sources, natural vegetation and subsistence at a high-altitude aboriginal settlement in Tenerife, Canary Islands: Micro-contextual geoarchaeological data from Roques de García Rock-shelter. *Archaeological and Anthropological Sciences*, 14(10), 195. <https://doi.org/10.1007/s12520-022-01661-9>
- Tsiplakou, E., Hadjigeorgiou, I., Sotirakoglou, K., & Zervas, G. (2011). Differences in mean retention time of sheep and goats under controlled feeding practices. *Small Ruminant Research*, 95, 48–53. <https://doi.org/10.1016/j.smallrumres.2010.09.002>
- Vallejo, A., Gea, J., Gorostizu-Orkaiztegi, A., Vergès, J. M., Martín, P., Sampedro, M. C., Sánchez-Ortega, A., Goicolea, M. A., & Barrio, R. J. (2022). Hormones and bile acids as biomarkers for the characterization of animal management in prehistoric sheepfold caves: El Mirador case (Sierra de Atapuerca, Burgos, Spain). *Journal of Archaeological Science*, 138, 105547. <https://doi.org/10.1016/j.jas.2022.105547>
- Vallejo, A., Gea, J., Massó, L., Navarro, B., Gorostizu-Orkaiztegi, A., Vergès, J. M., Sánchez-Ortega, A., Sampedro, M. C., Ribechini, E., & Barrio, R. J. (2022). Lipid biomarkers as a tool for the identification of herder activities in El Mirador Cave. In E. Allué, P. Martín, & J. M. Vergès (Eds.), *Prehistoric herders and farmers: A transdisciplinary overview to the Archeological record from El Mirador cave* (pp. 251–270). Springer International Publishing. [https://doi.org/10.1007/978-3-031-12278-1\\_13](https://doi.org/10.1007/978-3-031-12278-1_13)
- Vergès, J. M. (2011). La combustión del estiércol: aproximación experimental a la quema en montón de los residuos de redil. In A. Morgado, J. Baena, & D. García (Eds.), *La investigación experimental aplicada a la arqueología* (pp. 325–330). Universidad de Granada, Granada.
- Vergès, J. M., Burguet-Coca, A., Allué, E., Expósito, I., Guardiola, M., Martín, P., Morales, J. I., Burjachs, F., Cabanes, D., Carrancho, Á., & Vallverdú, J. (2016). The Mas del Pepet experimental programme for the study of prehistoric livestock practices: Preliminary data from dung burning. *Quaternary International*, 414, 304–315. <https://doi.org/10.1016/j.quaint.2016.01.032>
- Vidal-Matutano, P., Henry, A., Carré, A., Orange, F., & Théry-Parisot, I. (2021). Prehispanic fuel management in the Canary Islands: A new experimental dataset for interpreting *Pinus canariensis* micromorphological degradation patterns on archeological charcoal. *Review of Palaeobotany and Palynology*, 295, 104537. <https://doi.org/10.1016/j.revpalbo.2021.104537>
- Vidal-Matutano, P., Alberto-Barroso, V., Marrero, E., García, J. C., Pou, S., & Arnay de la Rosa, M. (2019). Vitriified wood charcoal and burnt bones from the pre-Hispanic site of Chasogo (Tenerife, Canary Islands, Spain). *Journal of Archaeological Science: Reports*, 28, 102005. <https://doi.org/10.1016/j.jasrep.2019.102005>
- Volkman, J. K., Barrett, S. M., Blackburn, S. I., Mansour, M. P., Sikes, E. L., & Gelin, F. (1998). Microalgal biomarkers: A review of recent research developments. *Organic Geochemistry*, 29, 1163–1179. [https://doi.org/10.1016/S0146-6380\(98\)00062-X](https://doi.org/10.1016/S0146-6380(98)00062-X)
- Weiner, S. (2010). *Microarchaeology: Beyond the visible archaeological record*. Cambridge University Press.
- Wiesenberg, G. L. B., Lehndorff, E., & Schwark, L. (2009). Thermal degradation of rye and maize straw: Lipid pattern changes as a function of temperature. *Organic Geochemistry*, 40, 167–174. <https://doi.org/10.1016/j.orggeochem.2008.11.004>
- Yang, H., & Sun, H. J. (2004). Crystal structure of a new phosphate compound, Mg<sub>2</sub>KNa(PO<sub>4</sub>)<sub>2</sub>·14 H<sub>2</sub>O. *Journal of Solid State Chemistry*, 177, 2991–2997. <https://doi.org/10.1016/j.jssc.2004.05.008>
- Yang, H., Sun, H. J., & Downs, R. T. (2011). Hazenite, KNaMg<sub>2</sub>(PO<sub>4</sub>)<sub>2</sub>·14-H<sub>2</sub>O, a new biologically related phosphate mineral, from Mono Lake, California, USA. *American Mineralogist*, 96, 675–681. <https://doi.org/10.2138/am.2011.3668>
- Yatabe, A., Vanko, D. A., & Ghazi, A. M. (2000). Petrography and chemical compositions of secondary calcite and aragonite in Juan de Fuca Ridge basalts altered at low temperature. *Proceedings ODP Science Results*, 168, 137–148.
- Yogev, U., Vogler, M., Nir, O., Londong, J., & Gross, A. (2020). Phosphorous recovery from a novel recirculating aquaculture system followed by its sustainable reuse as a fertilizer. *Science of the Total Environment*, 722, 137949. <https://doi.org/10.1016/j.scitotenv.2020.137949>
- Zech, M., Buggle, B., Leiber, K., Marković, S., Glaser, B., Hambach, U., Huwe, B., Stevens, T., Sümeği, P., Wiesenberg, G., & Zöller, L. (2010). Reconstructing Quaternary vegetation history in the Carpathian Basin, SE-Europe, using n-alkane biomarkers as molecular fossils: Problems and possible solutions, potential and limitations. *E&G Quaternary Science Journal*, 58, 148–155. <https://doi.org/10.3285/eg.58.2.03>

## SUPPORTING INFORMATION

Additional supporting information can be found online in the Supporting Information section at the end of this article.

**How to cite this article:** Fernández-Palacios, E., Jambriña-Enríquez, M., Mentzer, S. M., Rodríguez de Vera, C., Dinckal, A., Égüez, N., Herrera-Herrera, A. V., Mederos, J. F. N., Salas, E. M., Miller, C. E., & Mallol, C. (2023). Reconstructing formation processes at the Canary Islands indigenous site of Belmaco Cave (La Palma, Spain) through a multiproxy geoarchaeological approach. *Geoarchaeology*, 1–27. <https://doi.org/10.1002/gea.21972>